PERFORMANCE OF CONTAINMENT VESSEL UNDER SEVERE ACCIDENT CONDITIONS

SPE analysis meeting #3

March 27-29, 2012, Washington DC

SUMMARY

1. Global Behavior of the Containment Vessel LST (Model 3)
2. Modeling of the initial state
3. Permeability of the Containment Vessel
4. Rupture of linear seal (Model 2)

necs
Numerical Engineering & Consulting Services

Veronique LE CORVEC

Mahsa MOZAYAN KHARAZI

Charles GHAVAMIAN

EDF

Sylvie MICHEL-PONNELLE

Etienne GALLITRE

1. General Behavior of the fullscale SANDIA Model under LST

Objectives:

Application of the modeling assumptions from the Model 2 to the full-scale Sandia Containment Vessel.

Direct comparison with experimental results.

Studying for the global and local response.

Demonstration of the robustness of the model in modeling non-linear behavior of the structure.

Improvement since last study in 2005

Modeling assumptions :

Complete Model: Geometry (simplification for the openings)

Damage concrete law

Reinforcement : rebars

Prestressing tendons :

- ungrouted ducts
- grouted duct

Large Displacements assumption

Unstressed initial state

Results and conclusions :

Comparison of global and local response of the structure with experimental Data

Model geometry

Internal radius = 5.7 m

External radius = 5.375 m

Total Height= 22.5 cm

Number of Elements:
~ 18 000

Number of Elements
in the wall thickness:
~ 3/5 elements

Finer mesh for the
Openings:

- E/H Hatch
- A/L Hatch

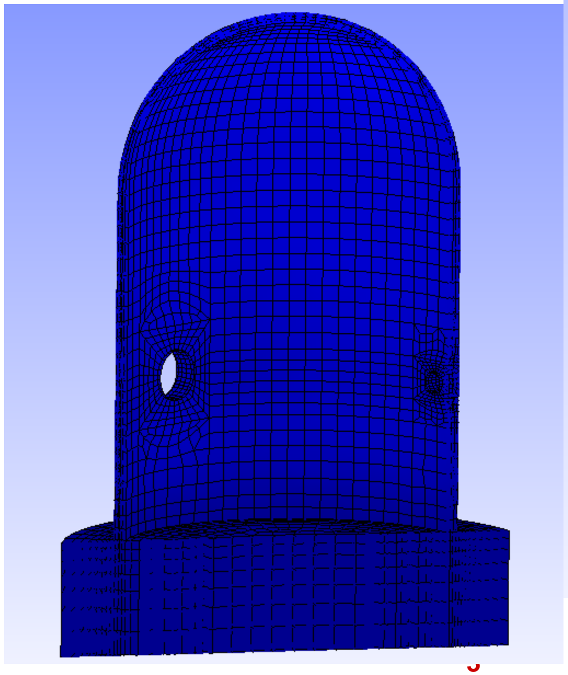

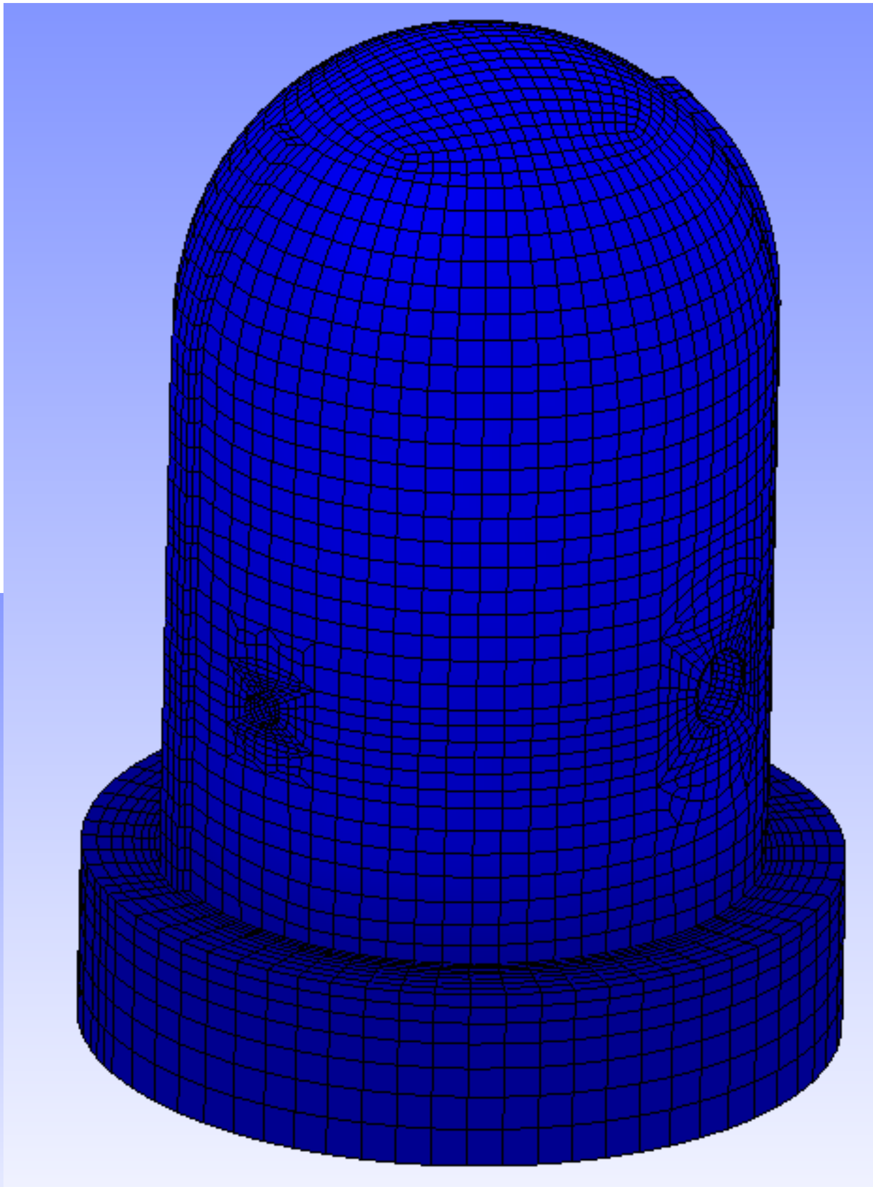

Components of the model :

Component	Element type	Material model
Concrete Structure	3D brick element	
Vessel, Dome		Concrete Damage law
Foundations, Buttress		Linear Elastic Material
Liner	2D plate element (DKT)	Plastic Material (VMIS)
Reinforcement bars	2D membrane element	
Prestressing tendons	1D elements Associated with 1D string element	Linear Elastic Material

Concrete constitutive model

MAZARS -> ENDO-ISOT

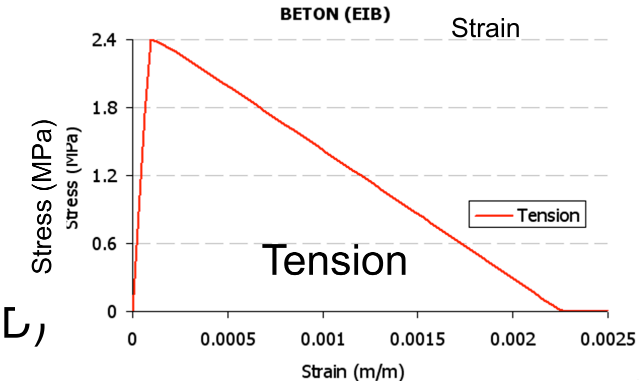

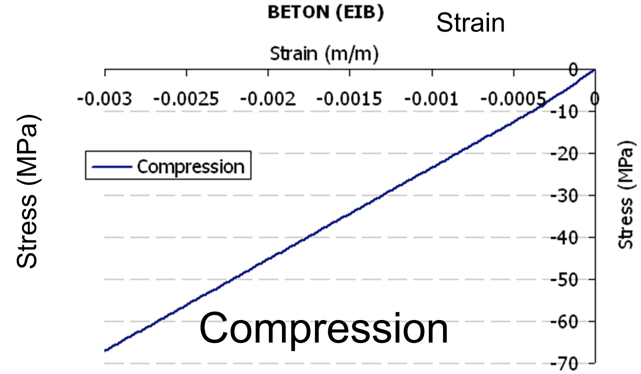

<u>Features :</u>

- Based on damage mechanics
- Limit in traction (tension / compression distinction)
- Linear response in compression
- Isotropic damage effect (single scalar damage index D)
- Crack reclosure

$$\sigma_{ij} = (1 - D) C_{ijkl} \, \varepsilon_{kl}$$

Parameter:

SYT = 2.4E6 , D_SIGM_EPSI = -1.0e9

Steel Reinforcement Layers

4 Reinforcement layers:
- INNER Vertical
- INNER Horizontal
- OUTTER Vertical
- OUTTER Horizontal

Identification of the density of reinforcement (steel area/ m) for the different zones.

8cm^2 /m< <29cm^2/m

Layers are defined on the inner and outter surface of the vessel, without eccentricity

Description des surfaces correspondant aux densités de ferraillage en cm²/m

9.8 :	1 2 16 24 25 35 47 55 85 92
13.5 :	3 4 17 18 26 27 56 57 62 81 86 93
18.1 :	12 36 39 48 51 65 66 76
20.5 :	5 6 7 13 19 20 21 28 29 30 37 40 42 49 52 58 59 60 63 64 67 68 77 78 82 83 87 88 94 95
28.9 :	8 9 10 14 15 22 23 31 32 33 38 41 46 50 53 54 61 69 75 79 80 84 89 90 96 97
49.3 :	11 34 91 98
40.9 :	71 73
57.7 :	72
34 :	43 45
49.3 :	44

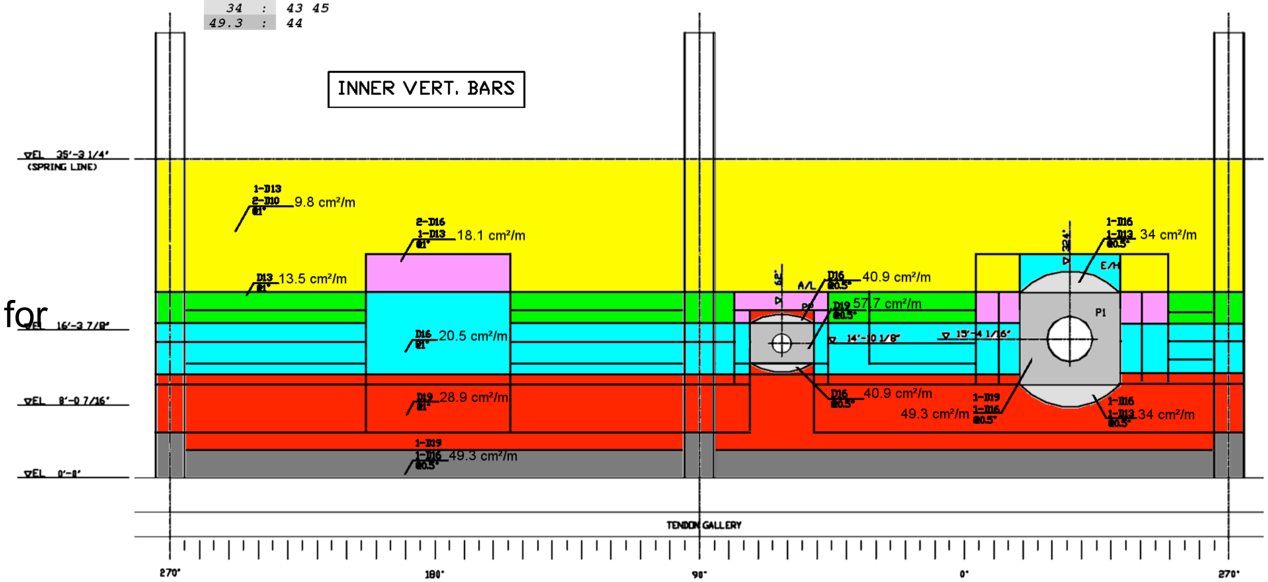

Non-linear elasto-plastic model:

Behaviour law: Non linear elasto-plastic
GRILLE_ISOT_LINE
Parameters: SY= 445.0E6 , D_SIGM_EPSI = 1250.0E6

Prestressing Tendons

Modeling of the complete set of ~180 cables
With finer mesh

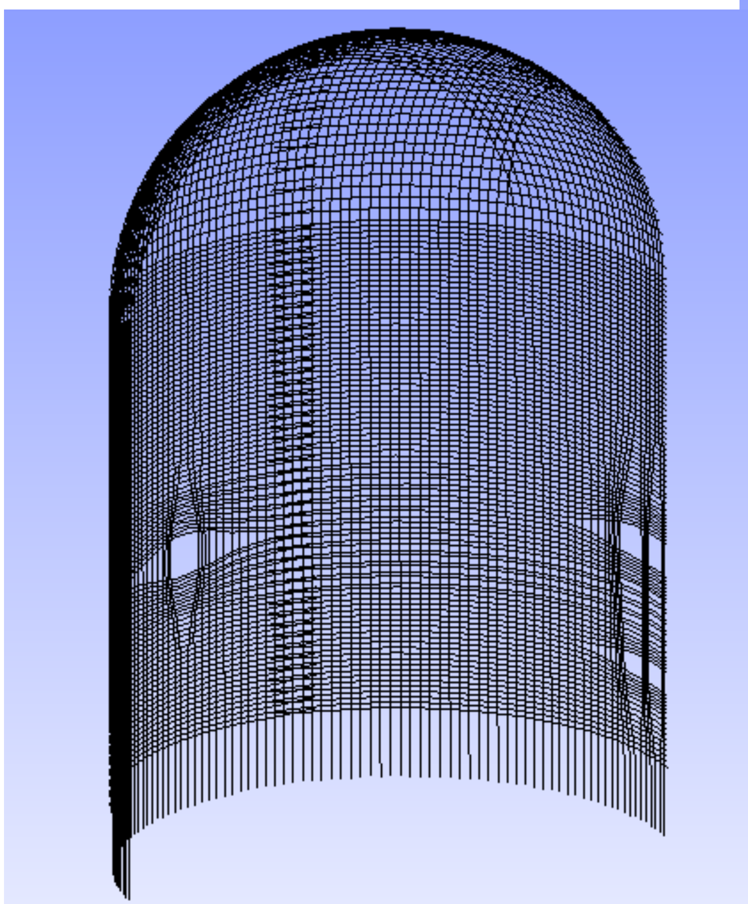

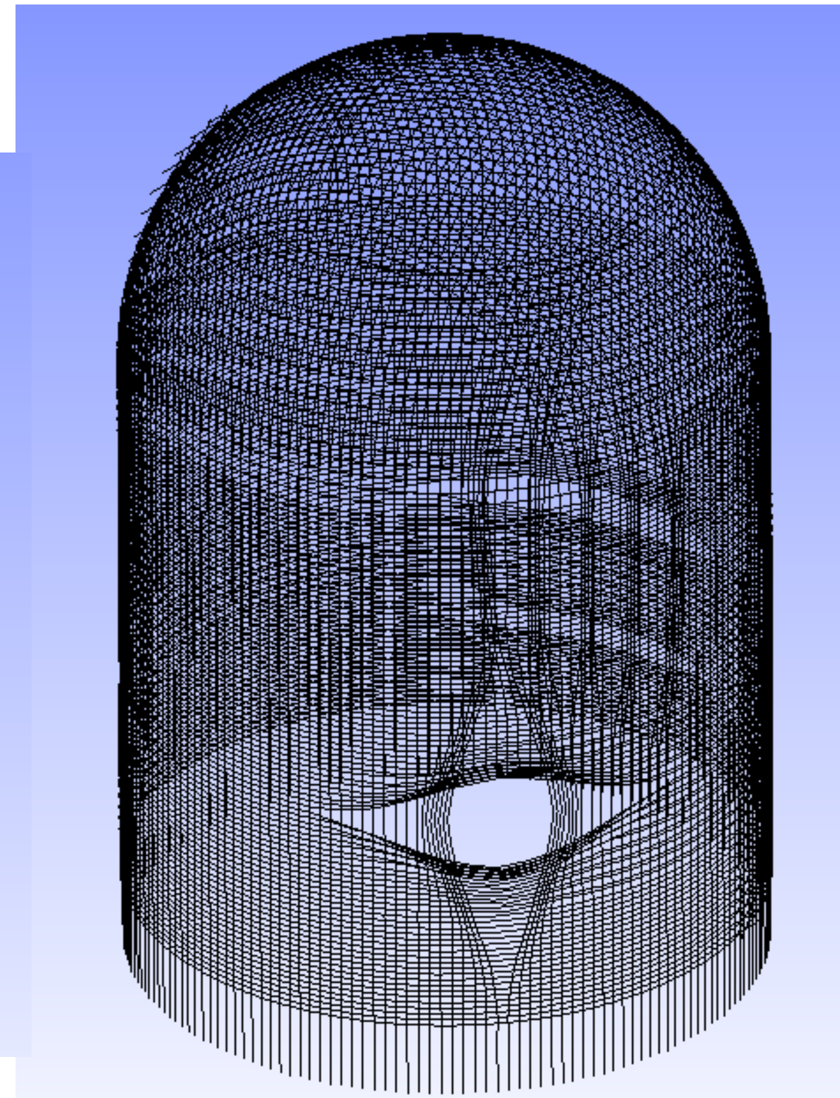

Tendon steel constitutive model

Elastoplastic

Parameters:

Young Modulus in elastic phase (E) = 191 000 MPa

Young Modulus in plastic phase (E) = 5 894 MPa

Poisson's ratio (ν) = 0.3

Density (ρ) = 7850 kg/m3

Yield Strength (Y_s) = 1 679MPa

Tensile Strength (XXX) = 1 856.76 MPa

Density (ρ) = 7850 kg/m^3

Angular and wobble friction: μ =0.21; λ = 0.001

Tendons section = 3.393 cm² (each tendon)

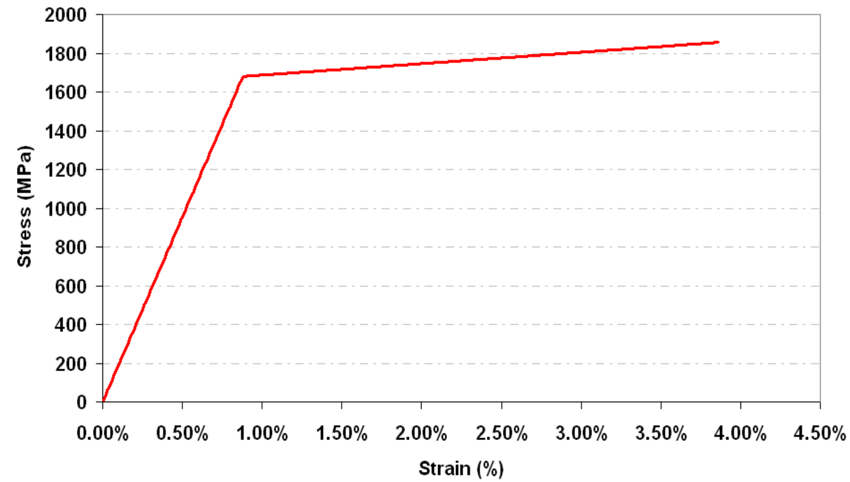

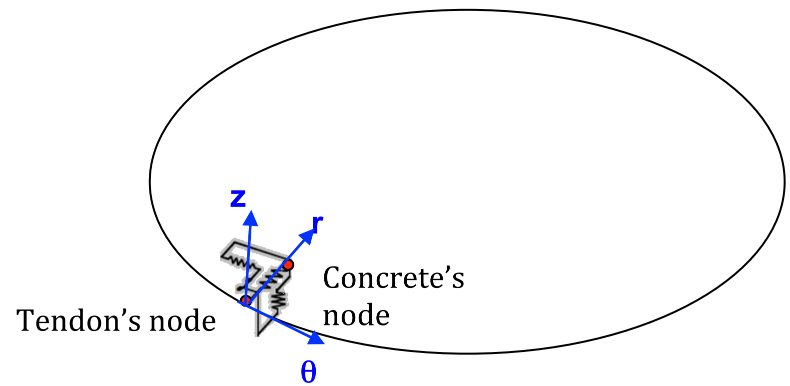

Ungrouted Model

(perfectly bonded in Z and R direction, friction along tendon direction)

Coefficient for bonding kx,ky,kz =1e9

Prestressing Loading:

- Initial Prestressing Force — Hoop Tendons = 43.21t; Vertical Tendons =48.02 t
- Setting Losses — Hoop Tendons = 0.00395; Vertical Tendons = 0.005

Results

- Global structural Behavior: deformed shape
  Comparison radial and vertical displacement with experimental results

- Damage evolution in the Vessel

- Evolution of the axial force in the prestressing tendons

- Response of the Liner

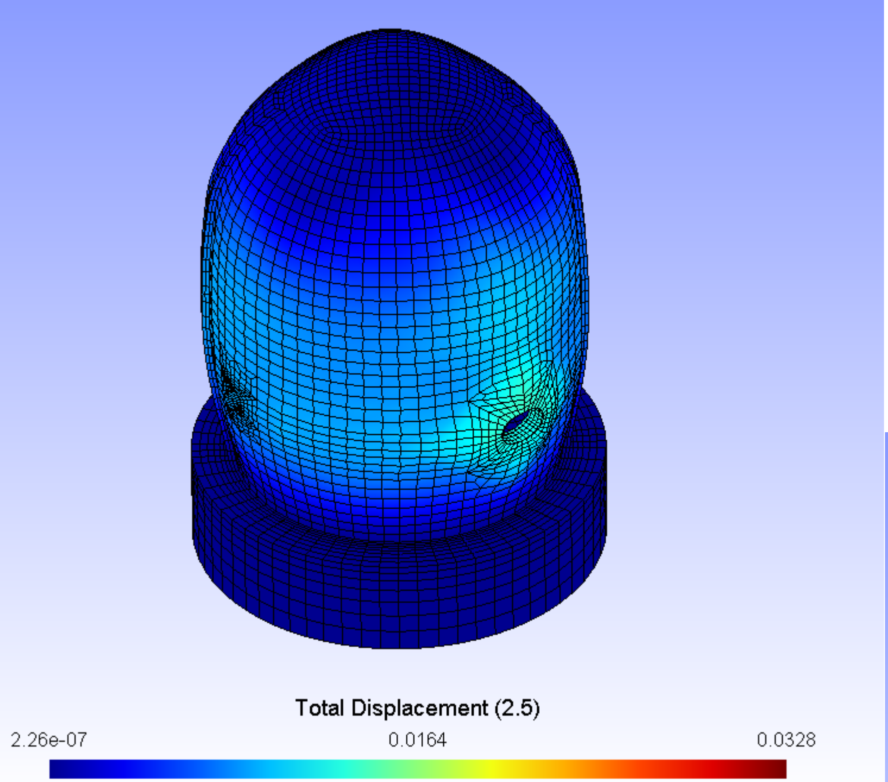

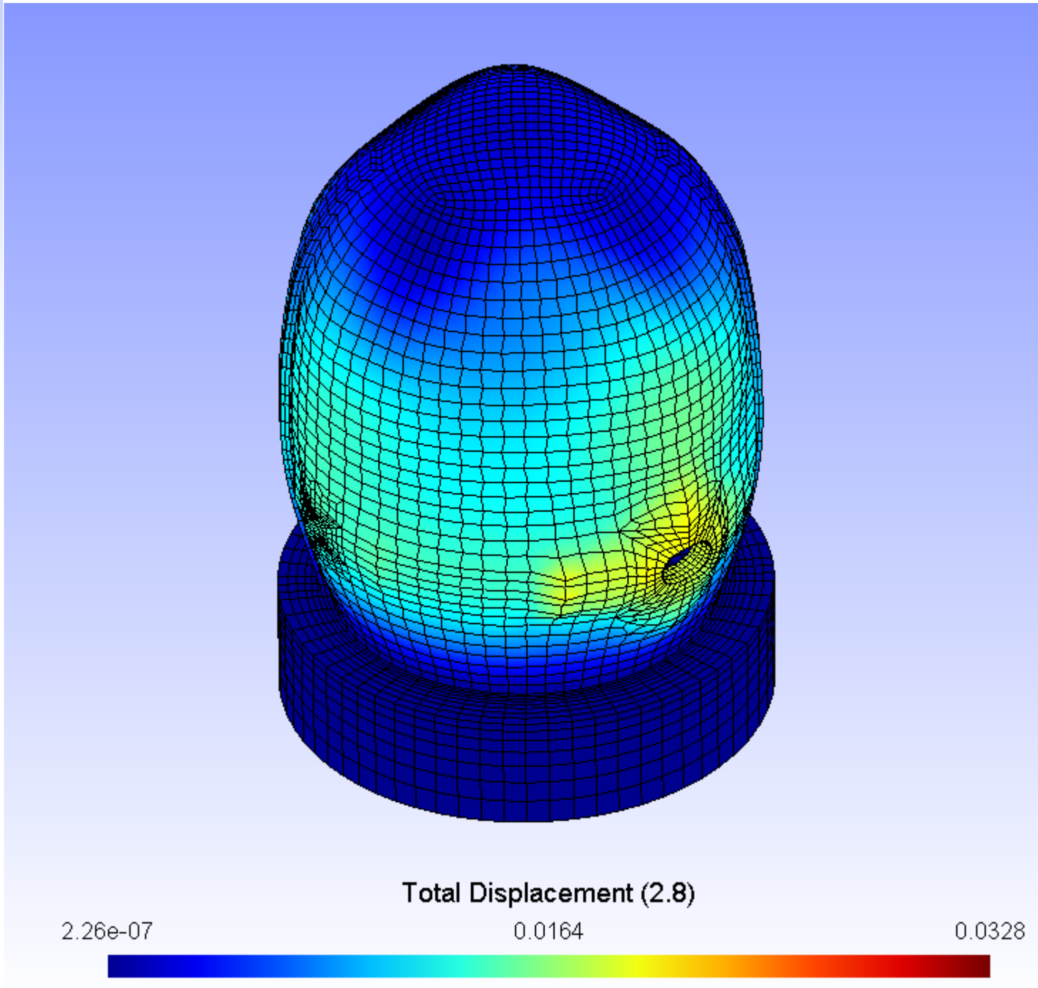

Magnification Factor =100
Values in meters

A1

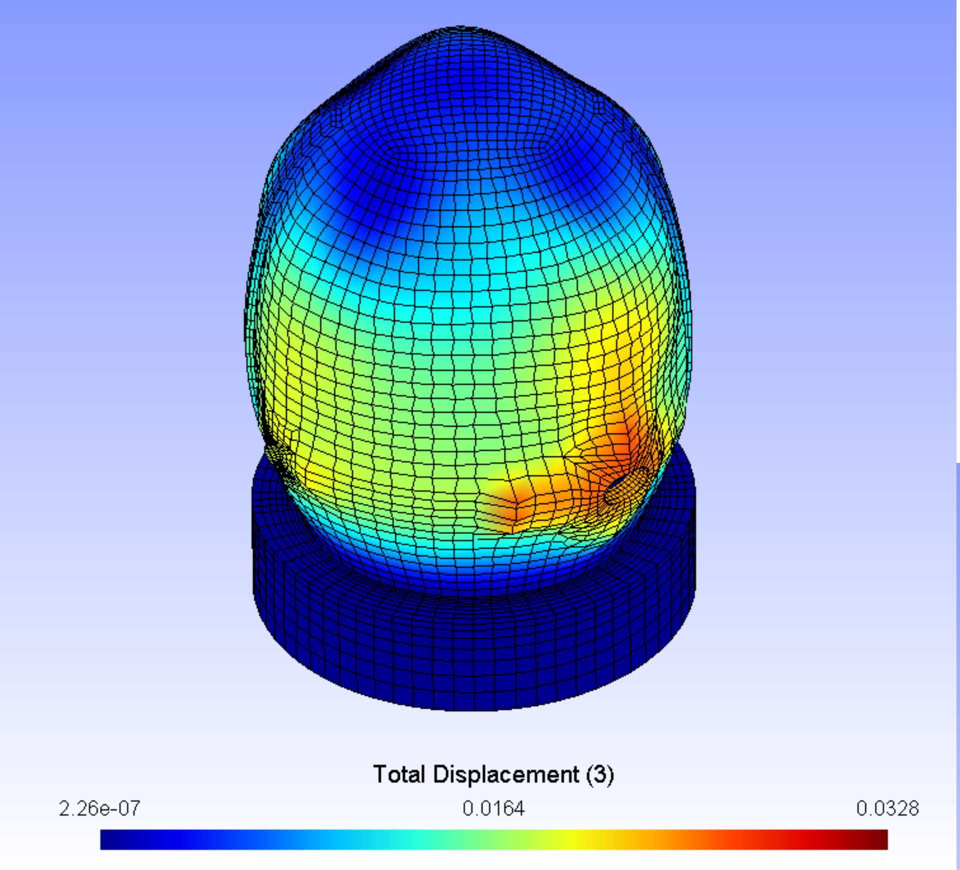

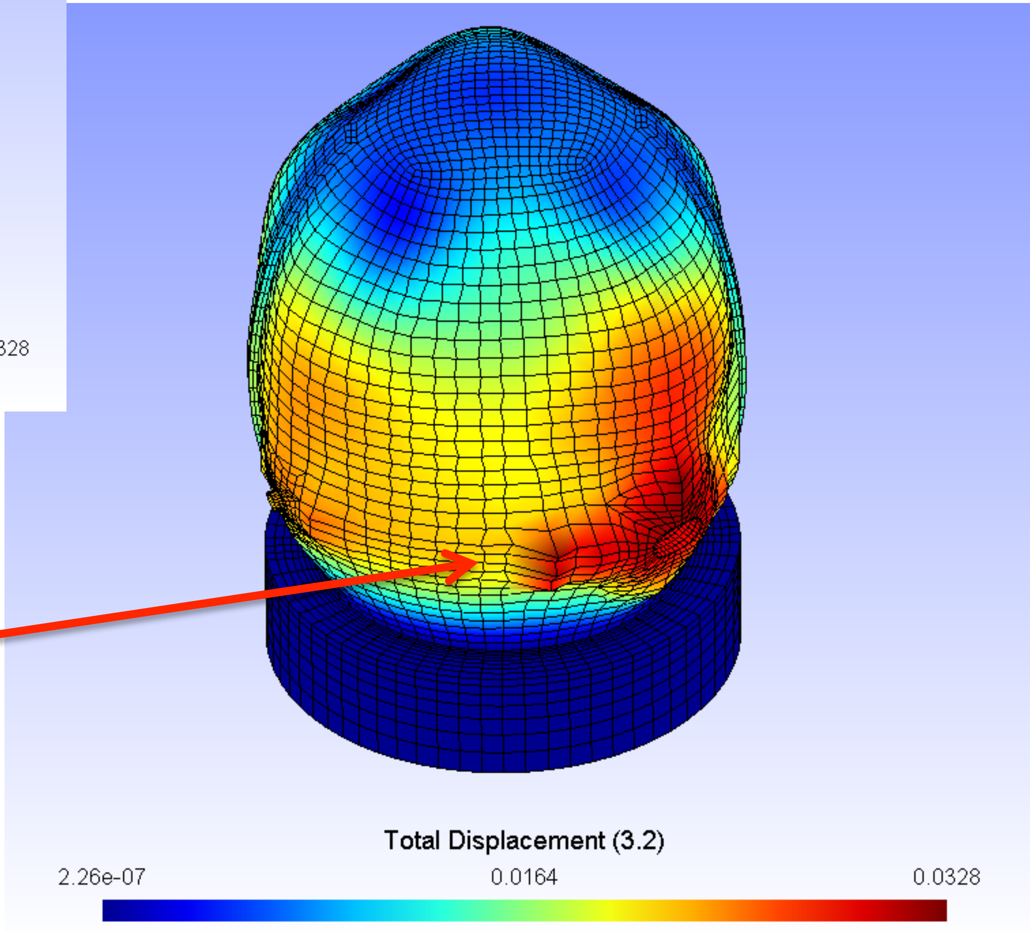

'Discontinuity in deformed shape'

Magnification Factor =100

A1 Values in meters

Radial Displacements

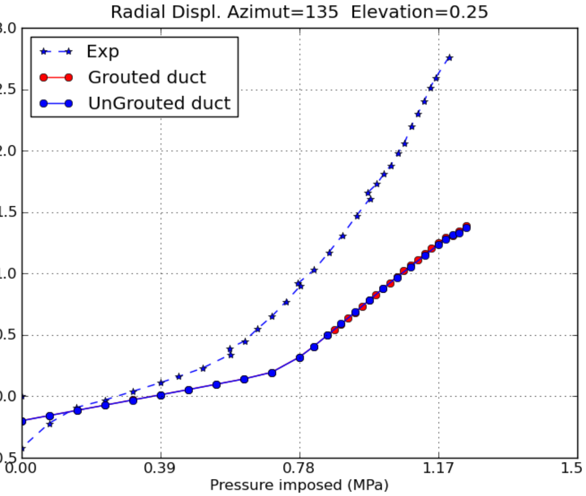

Z=0.25m

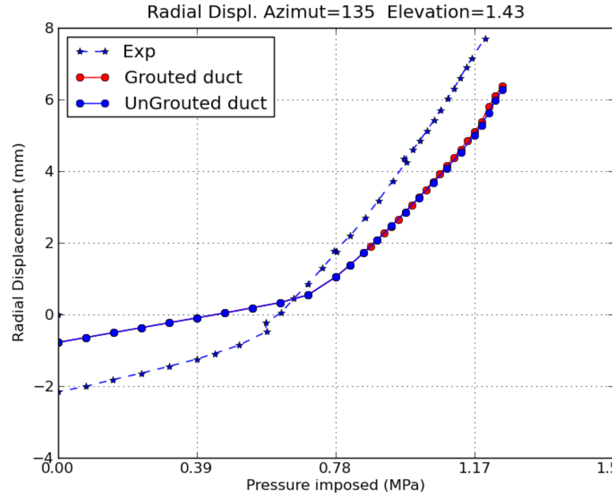

Z=1.43m

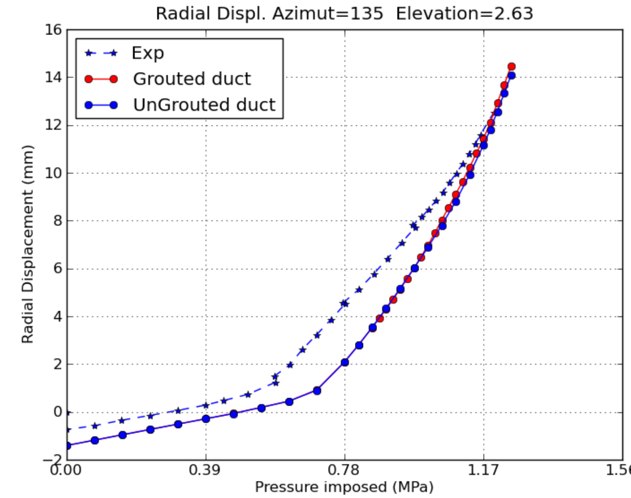

Z=2.63m

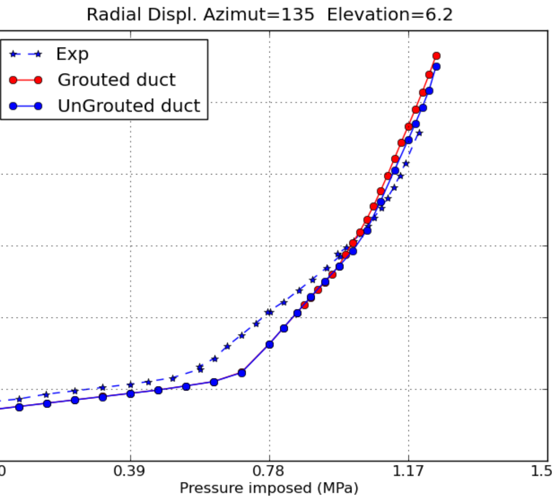

Z=6.2m

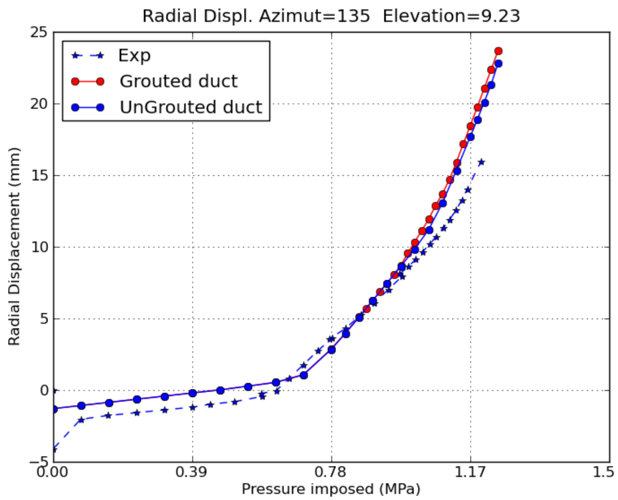

Z=9.23m

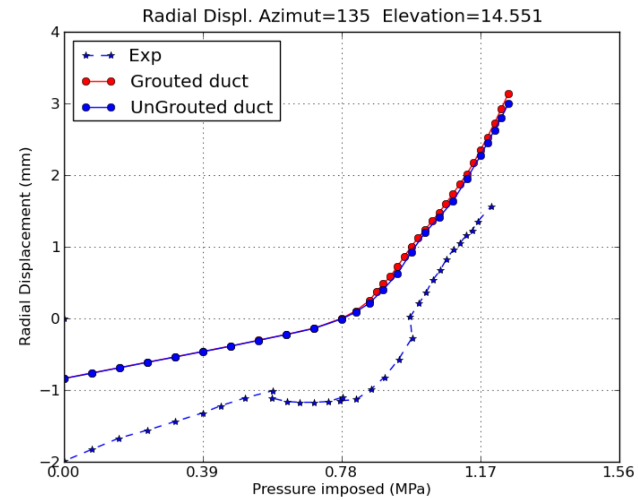

Z=14.55m

Vertical Displacements

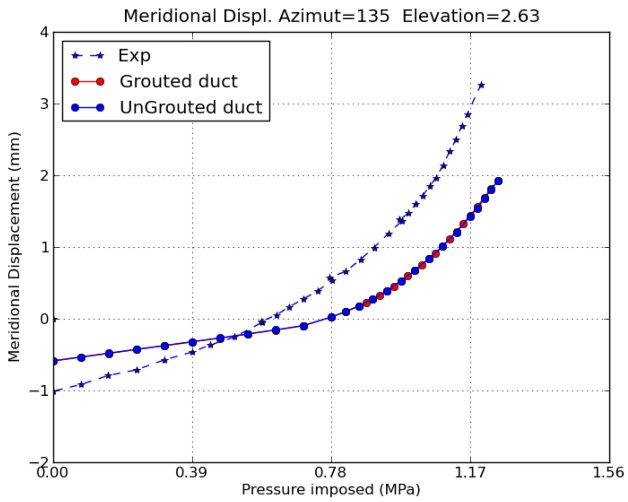

Z=2.63m

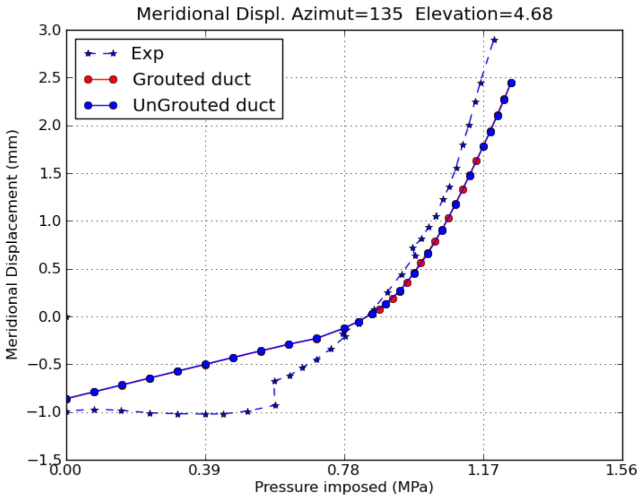

Z=4.68m

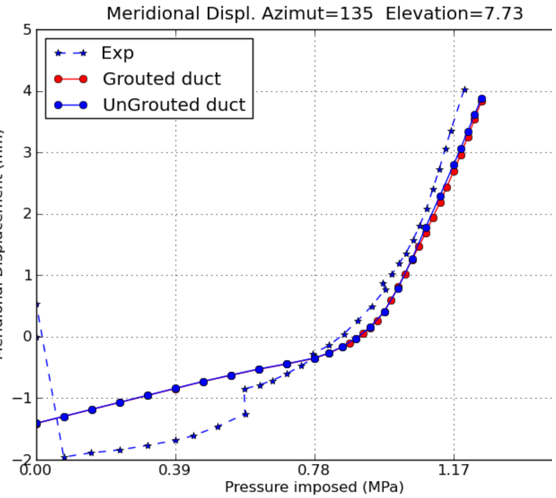

Z=7.73m

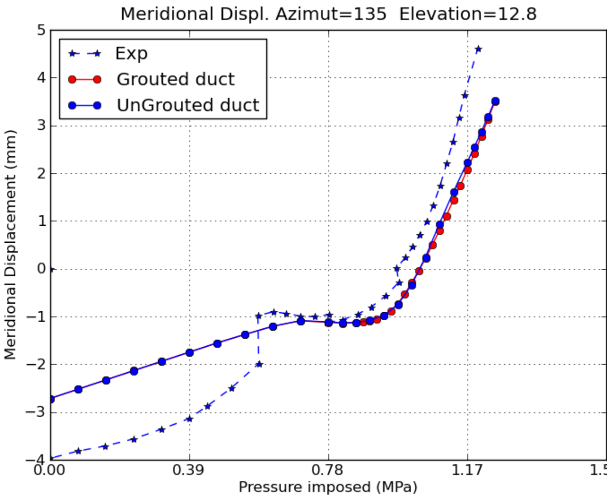

Z=12.8m

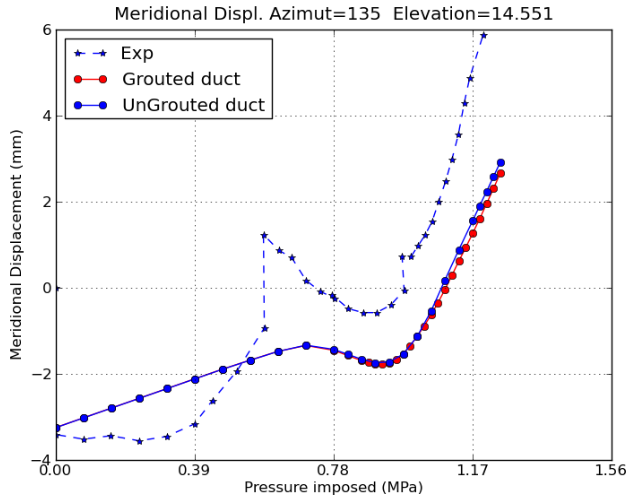

Z=14.55m

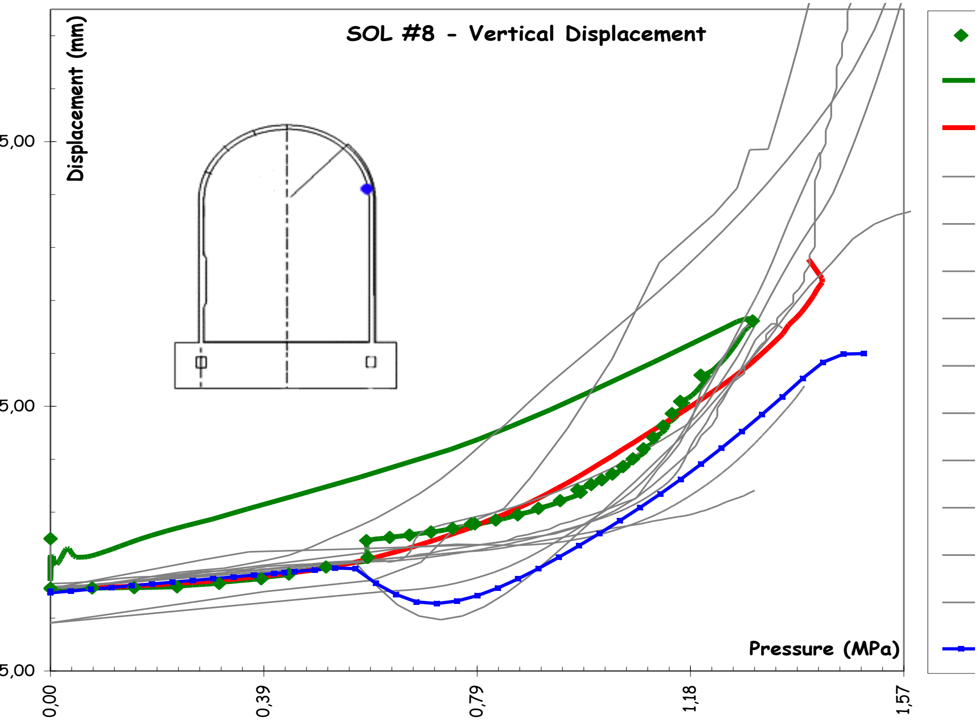
SOL #8 - Vertical Displacement
Displacement (mm)
Pressure (MPa)
5,00
5,00
5,00
0,00
0,39
0,79
1,18
1,57

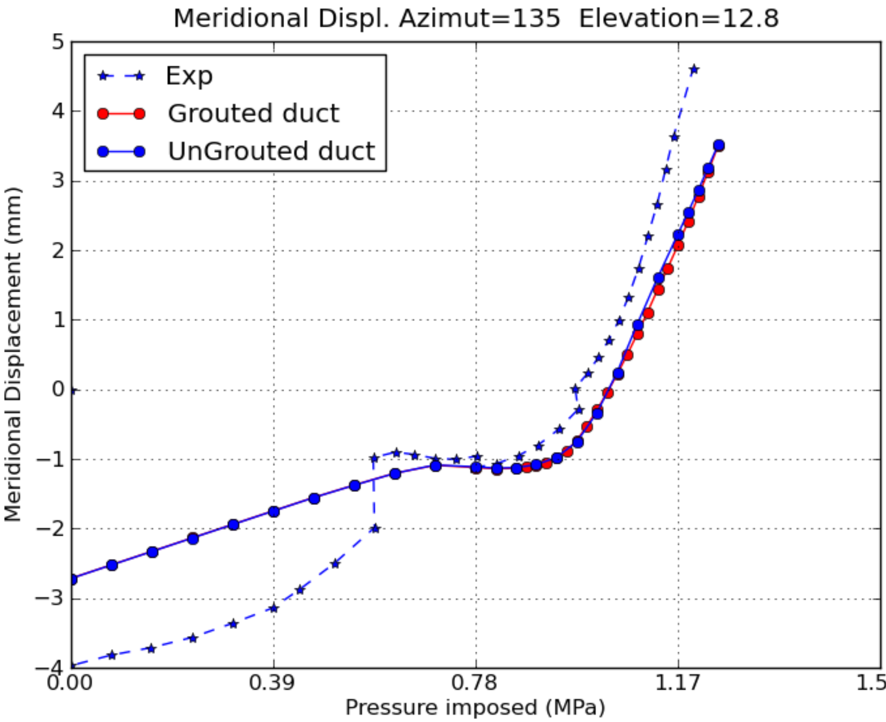
Meridional Displ. Azimut=135 Elevation=12.8
Exp
Grouted duct
UnGrouted duct
Meridional Displacement (mm)
Pressure imposed (MPa)
5
4
3
2
1
0
−1
−2
−3
−4
0.00
0.39
0.78
1.17
1.5

Effect of small displacements/ versus Updated geometry

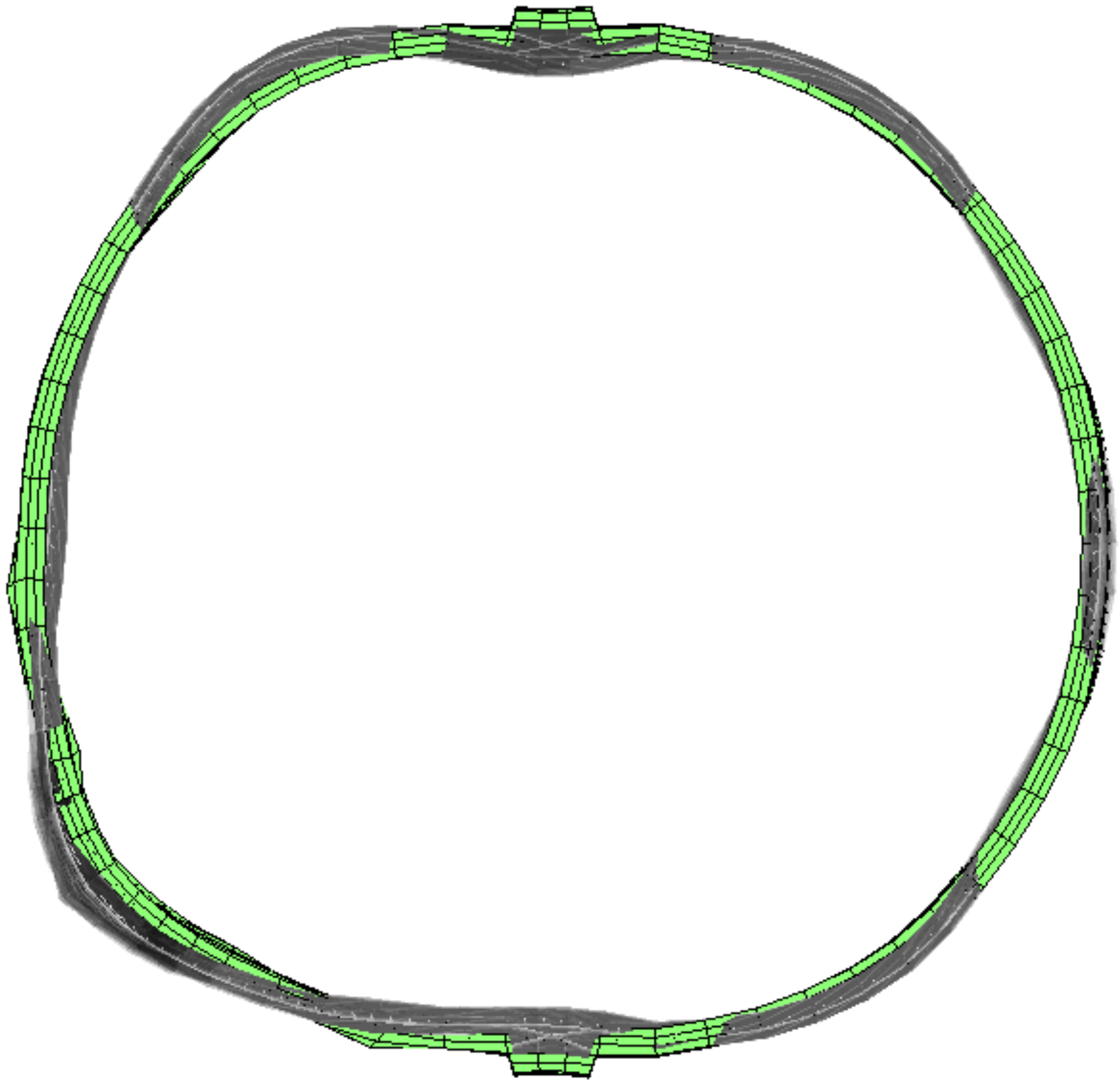

A1

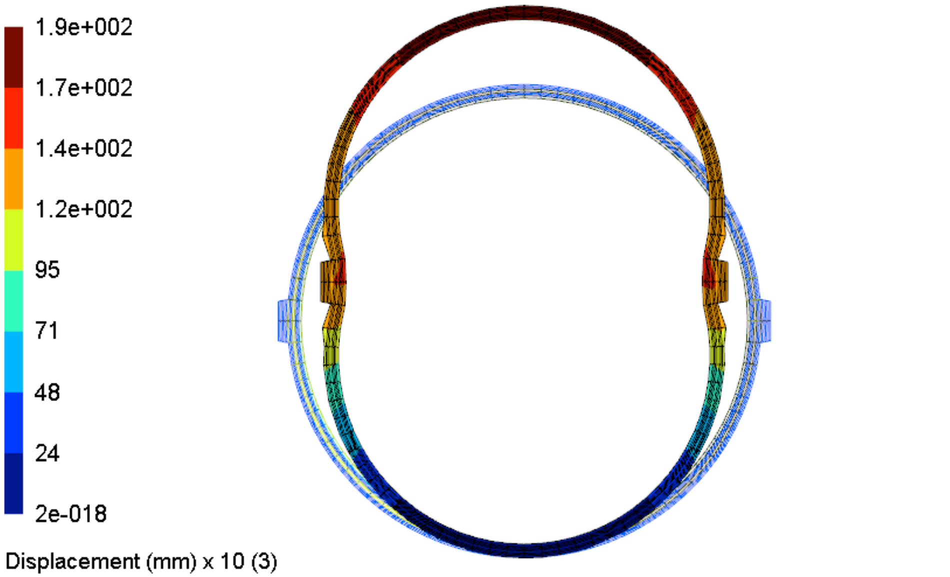

Deformed shape with small displacement assumption

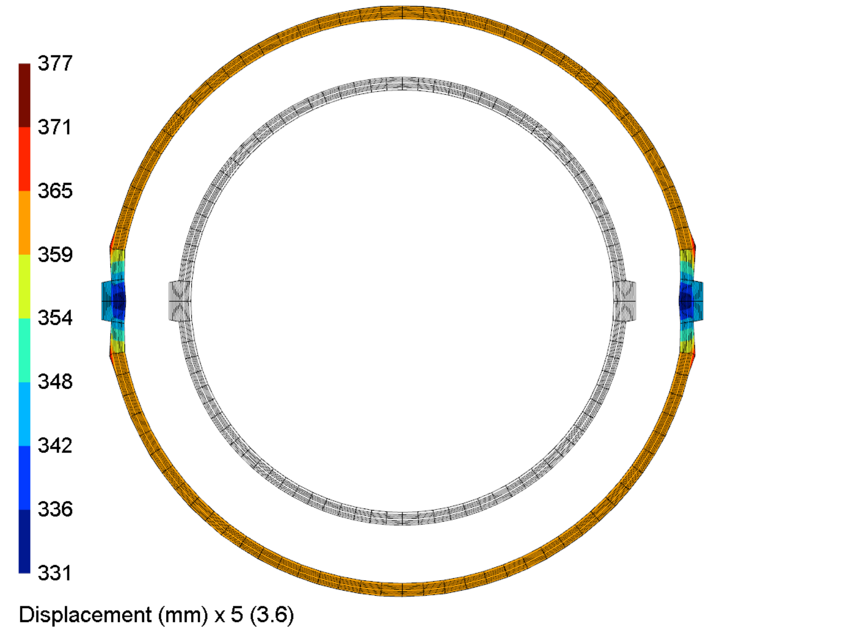

Deformed shape with updated geometry
P = 3.6 x pd= 1.40 MPa - Magnification factor: 5

Spread of damage in the concrete elements

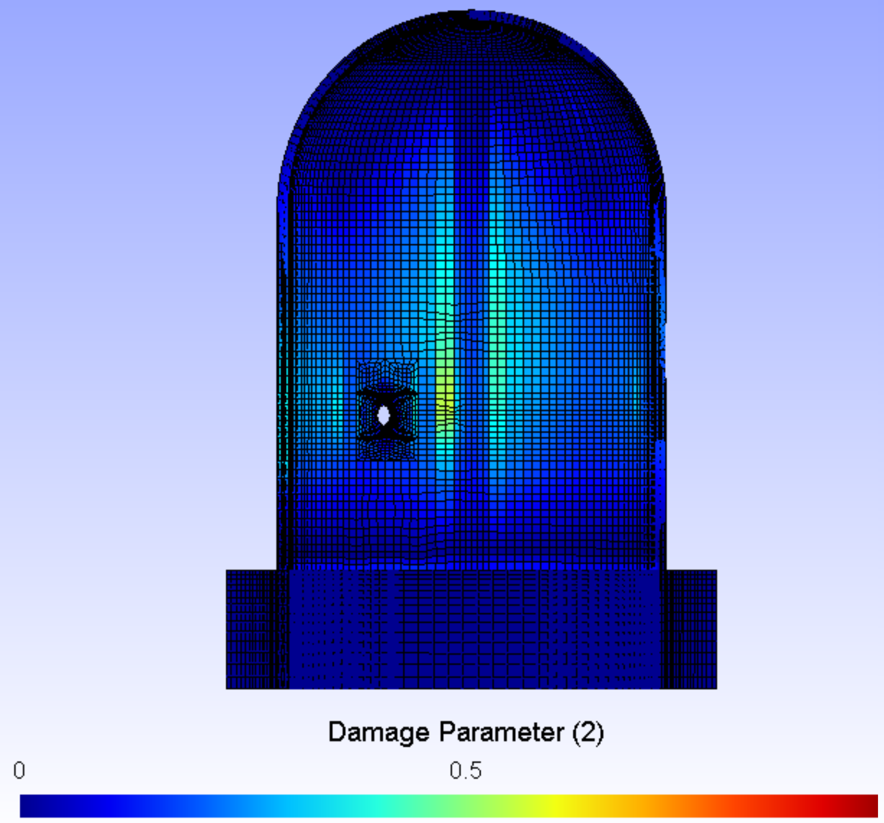

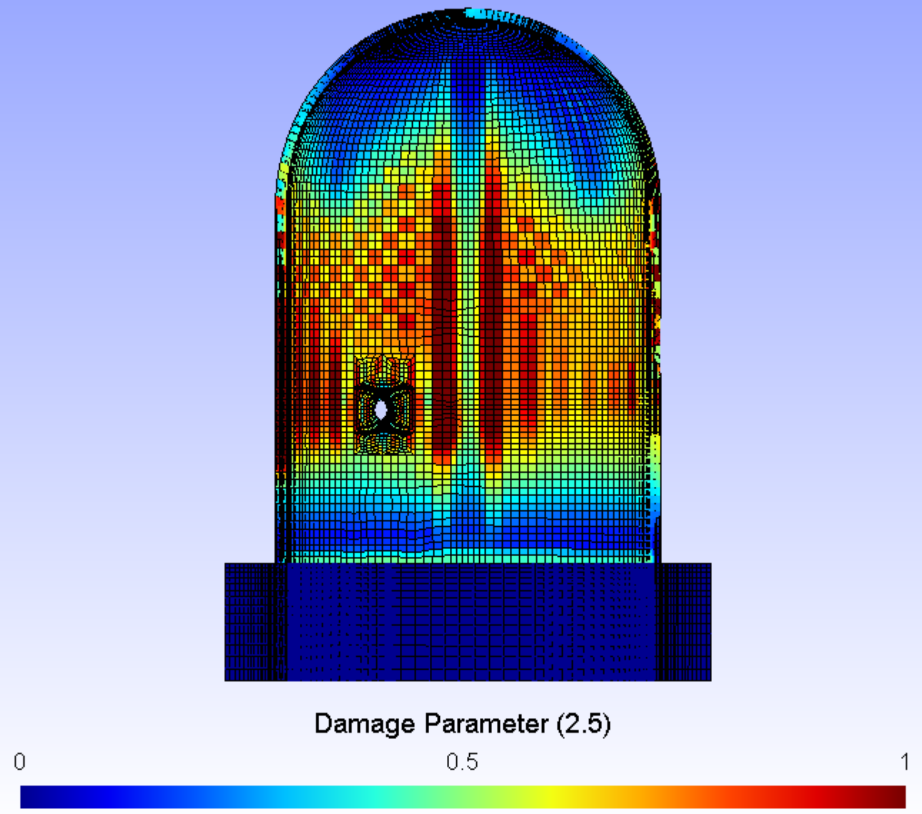

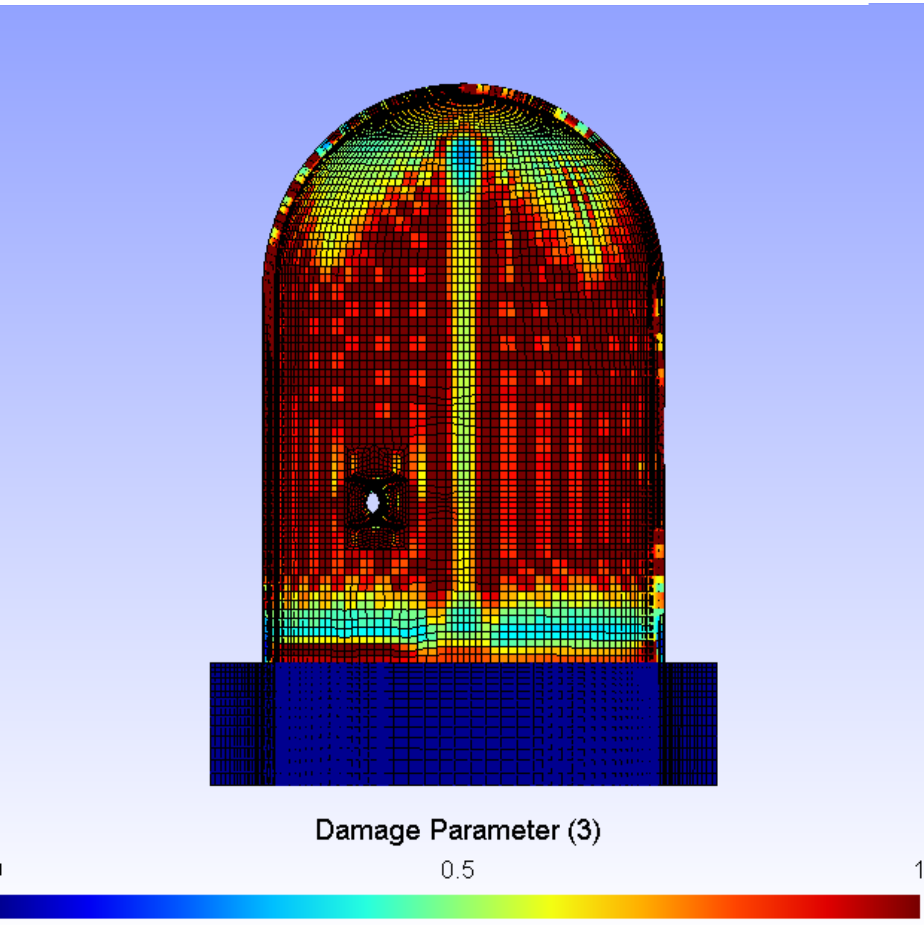

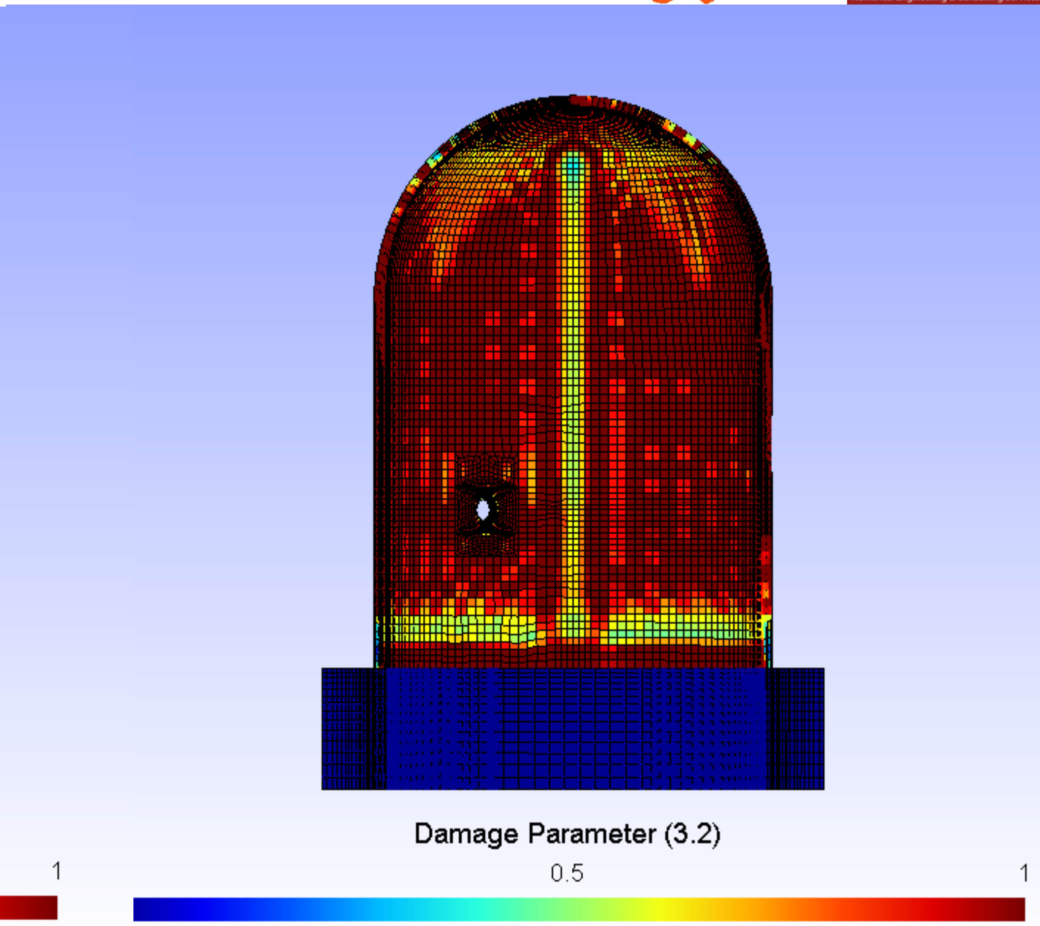

P =3.2Pd

Liner Response

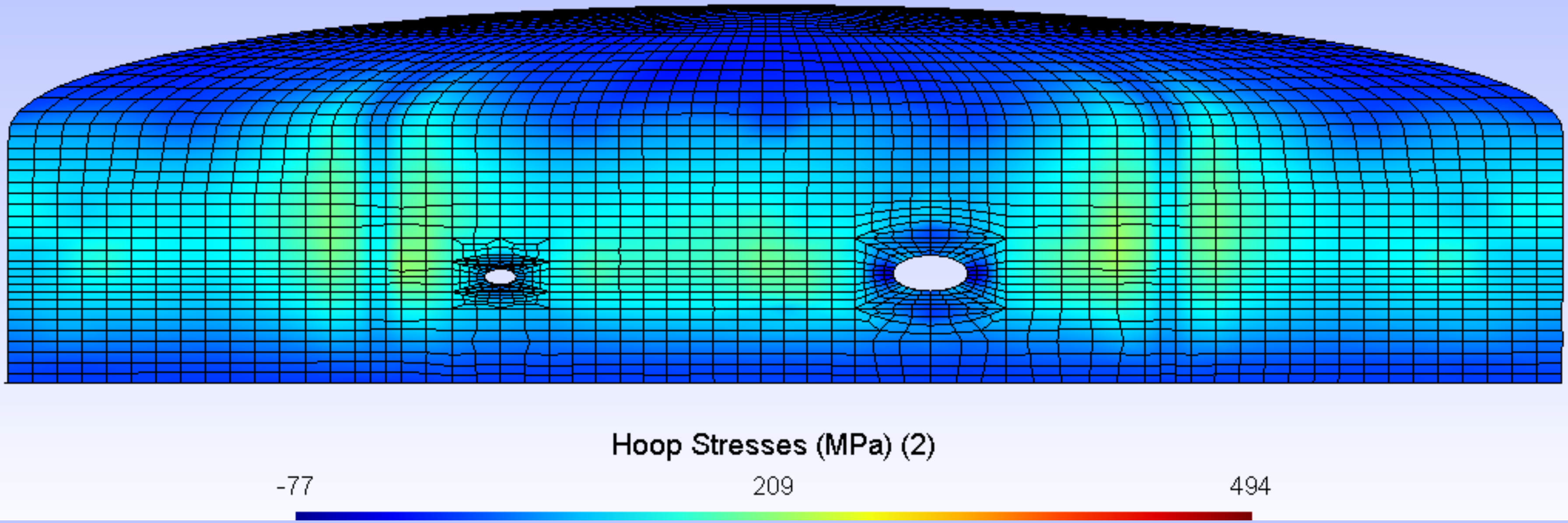

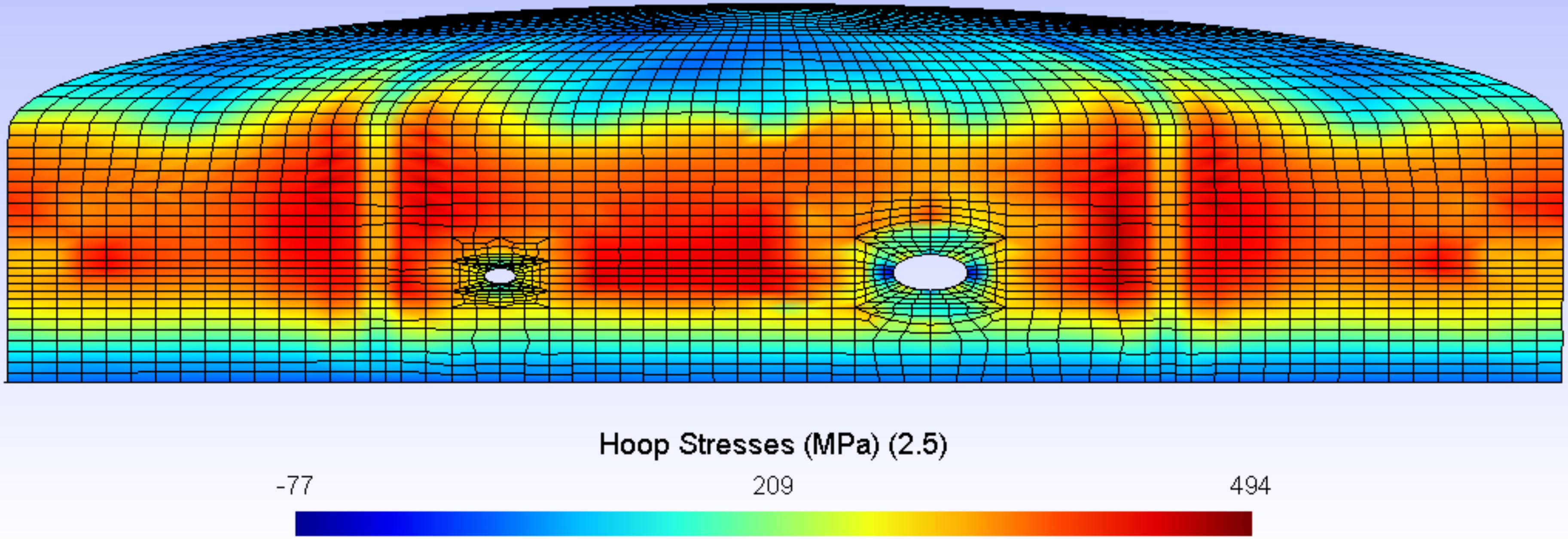

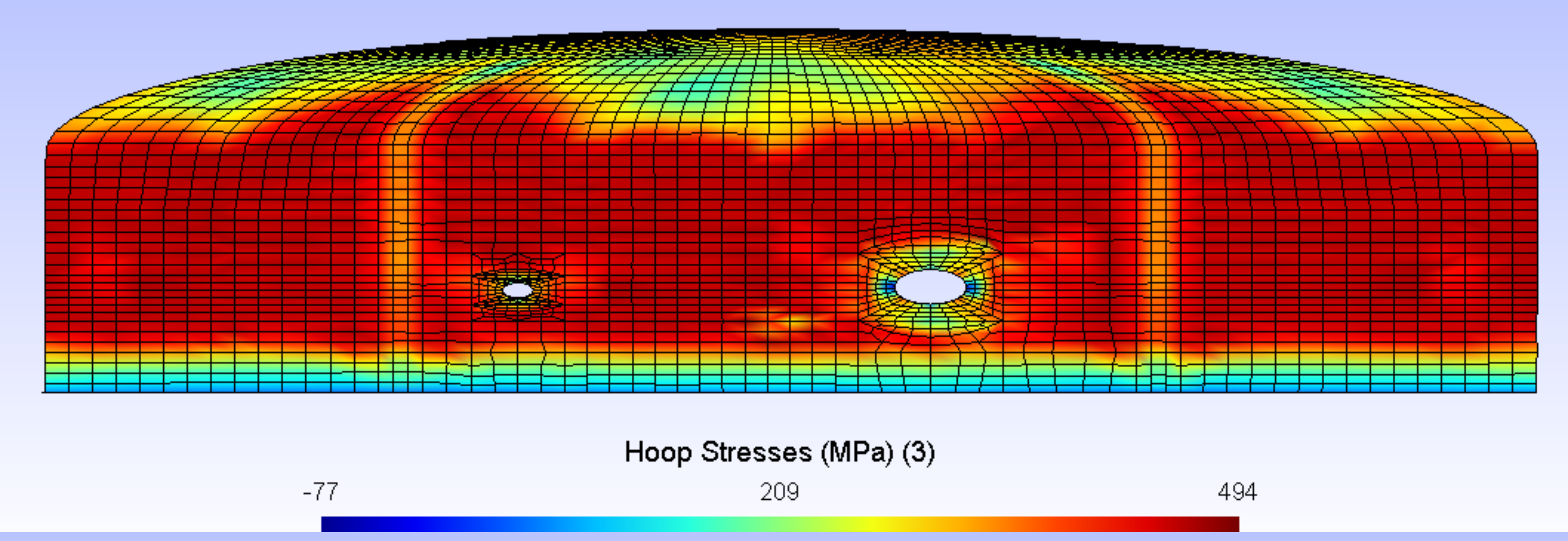
Hoop Stresses (MPa) (3)
-77
209
494

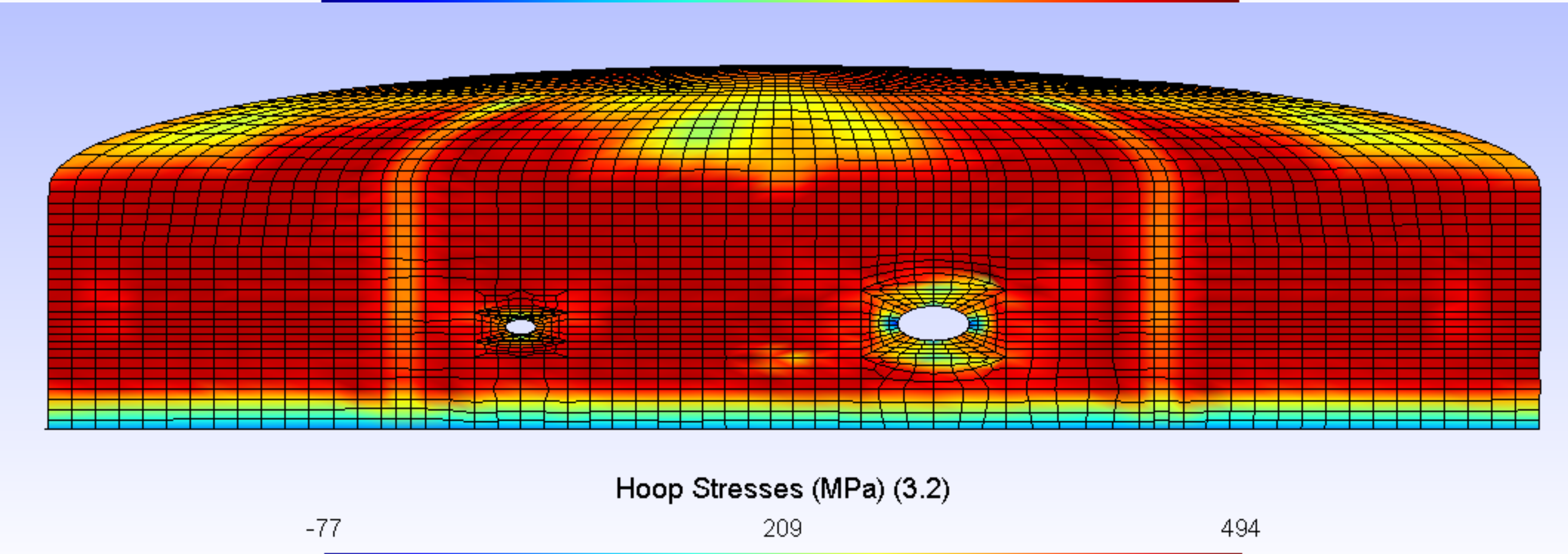
Hoop Stresses (MPa) (3.2)
-77
209
494

Tendons Response

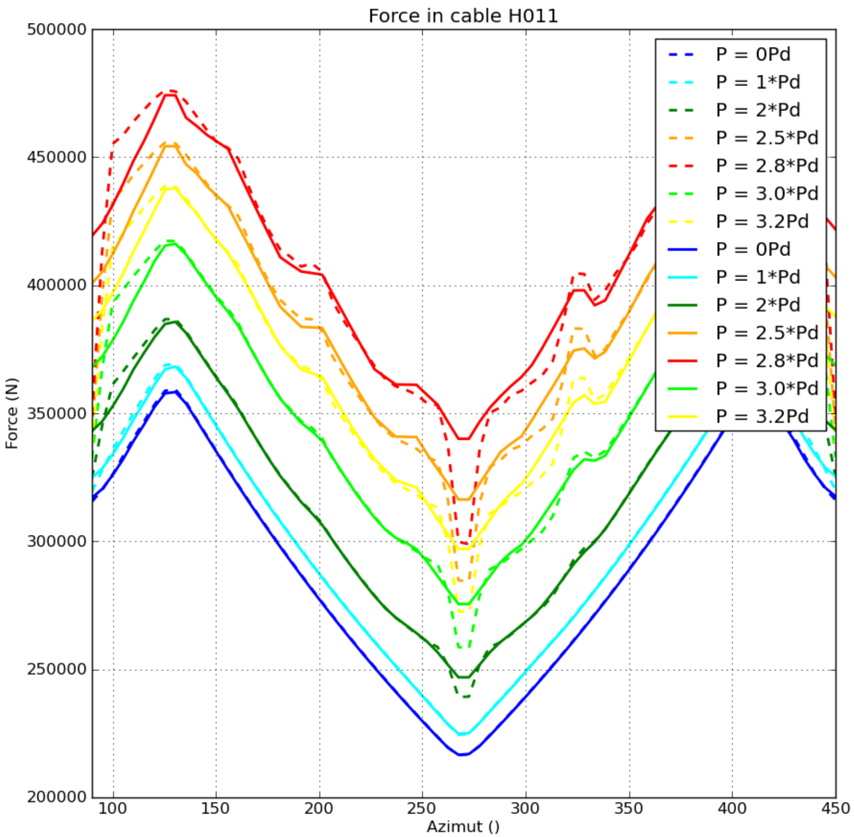

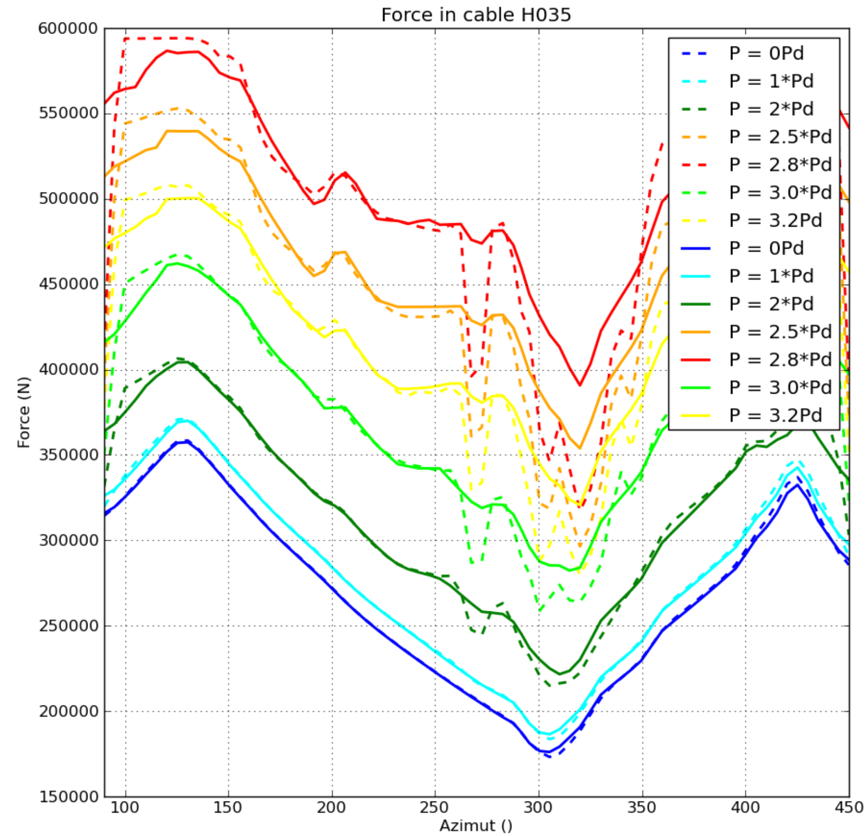

Ungrouted tendon (plain line)

Grouted tendon (dotted line)

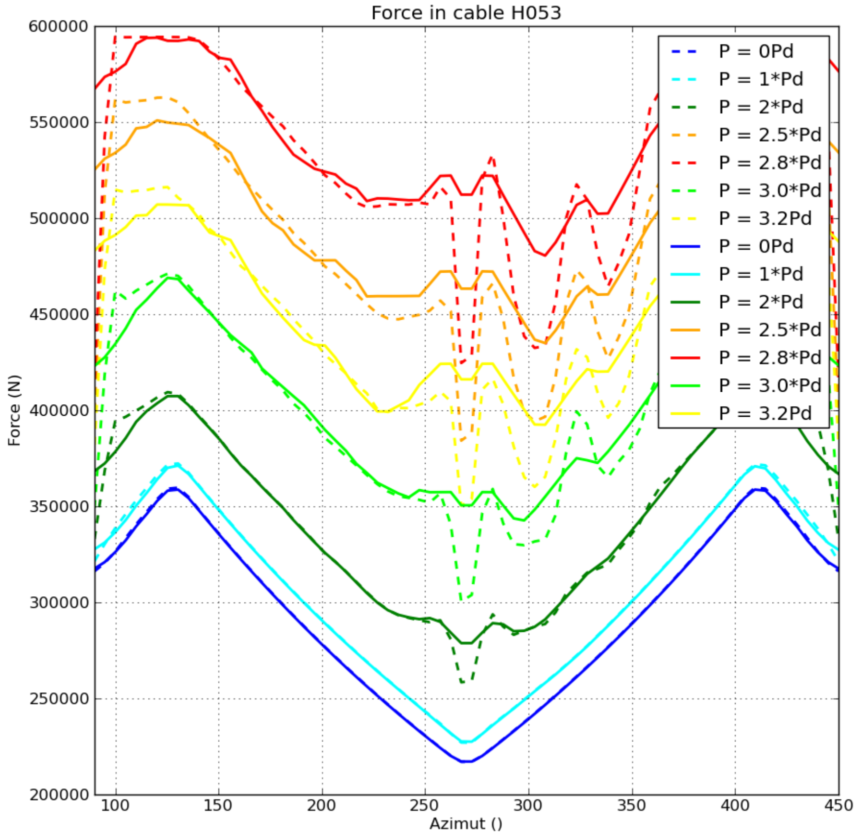

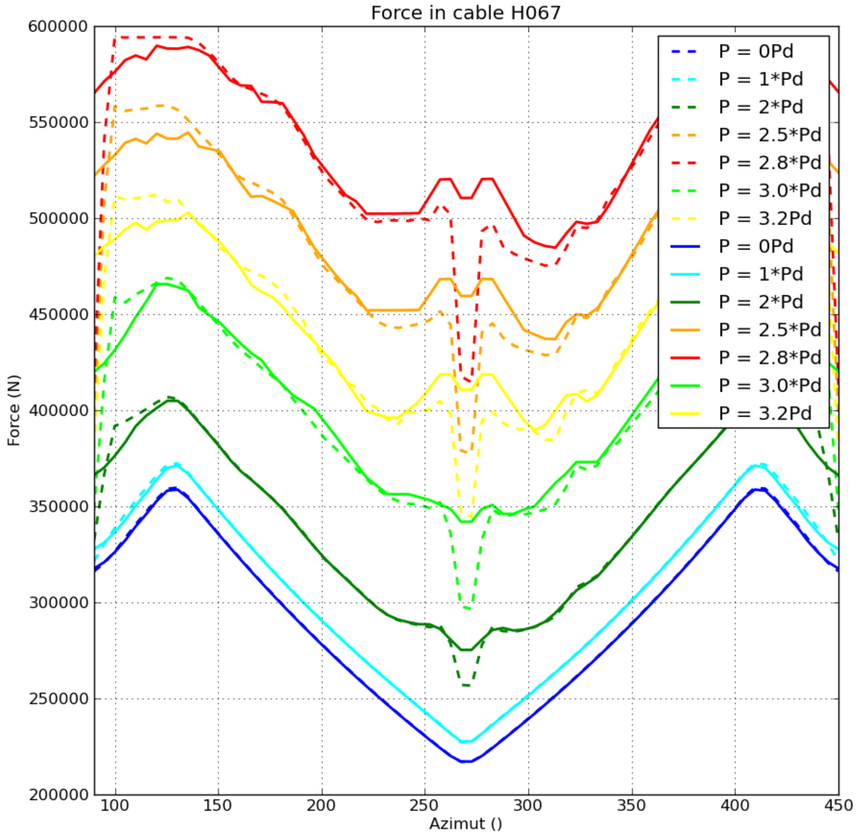

Ungrouted tendon (plain line)

Grouted tendon (dotted line)

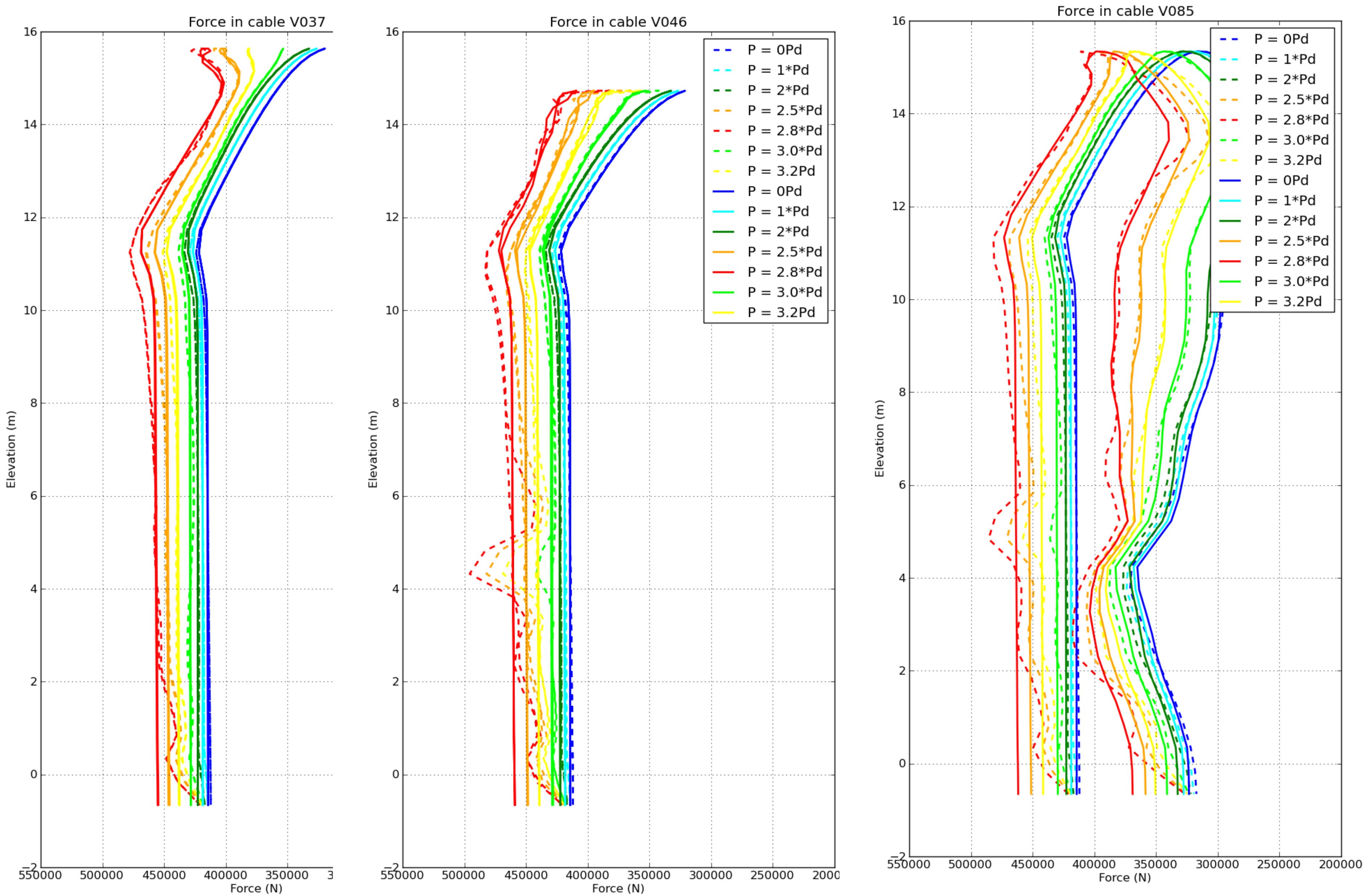

Ungrouted tendon (plain line)

Grouted tendon (dotted line)

Conclusions:

- Good estimation of the global behavior of the structure.
- Better estimation in the central Vessel (far from foundations and dome)
- Negligible Effect on the tendons modeling on the global response
- Noteworthy effect of the choice of updated geometry for the calculation
  (updated geometry 'PETIT REAC')
- Comparison of the Grouted or Ungrouted cable modeling:
  smoothening of the response (axial force) close to the openings.

2. Initial State

Objective :
How to model / account for the different lifts and its effects on the structural response of the structure (short term / long term)

Modeling :
Full-scale structure at three successive construction state
Reinforcement rebars and tendons not accounted for in the model

Concrete behavior Modeling

- Thermal effects: $\varepsilon_{T°}$: cooling of the concrete (ΔT = 40°C)
- Autogeneous effects : $\varepsilon_{autogeneous°}$: according to EC2
- Creep effects: $\varepsilon_{creep°}$: according to EC2

Model Assumption

Modeling :

Full-scale structure at three successive construction state

3d brick elements , quadratic mesh for mechanical part

Reinforcement rebars and tendons not accounted for in the model

	Concrete Pour	Specified Strength
	Date	f_c' (kg/cm^2)
F1	2-12-97	300
F2	2-28-97	300
F3A	5-8-97	300
F3B	5-8-97	450
F4	7-2-97	450
C1	11-11-98	450
C2	12-10-98	450
C3	1-5-99	450
C4	1-28-99	450
D1	3-3-99	450
D2	4-12-99	450
D3	4-15-99	450
F5	5-24-00	300
F6	6-9-00	450

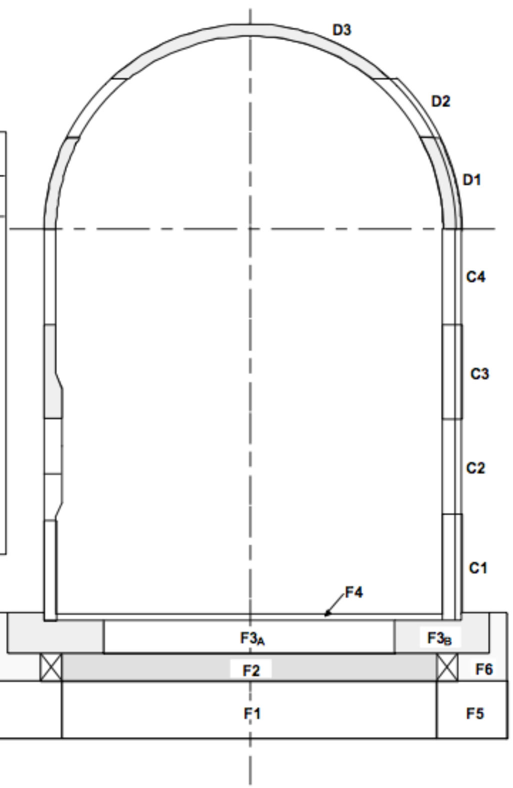

Figure 2.7 PCCV Concrete Lifts and Strengths

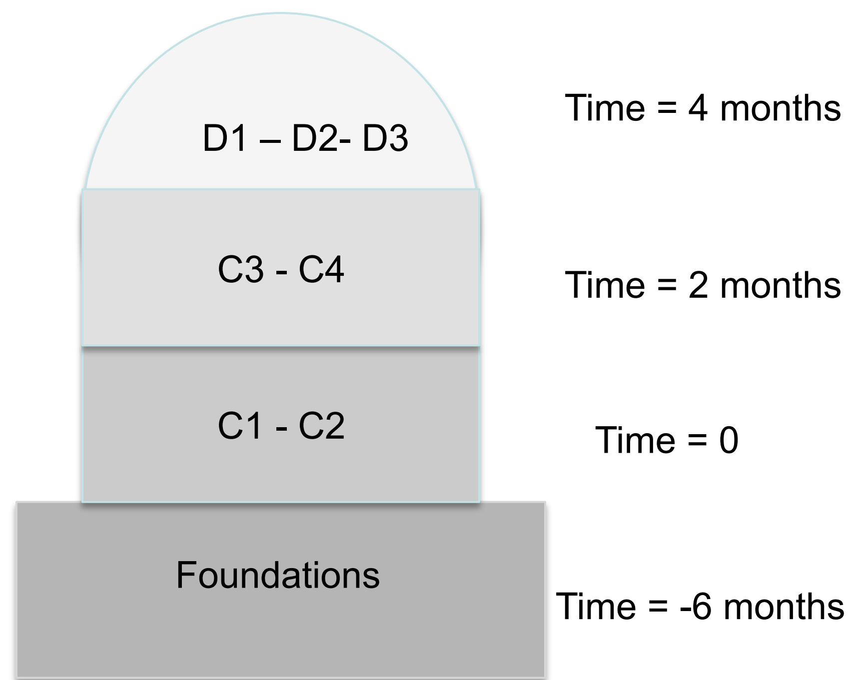

Concrete behavior Modeling

- Thermal effects: $\varepsilon_{T°}$: cooling of the concrete (ΔT = 40°C)
- Concrete Hydration (Hardening) : according to EC2
- Autogeneous effects : $\varepsilon_{autogeneous°}$: according to EC2
- Creep effects: $\varepsilon_{creep°}$: according to EC2

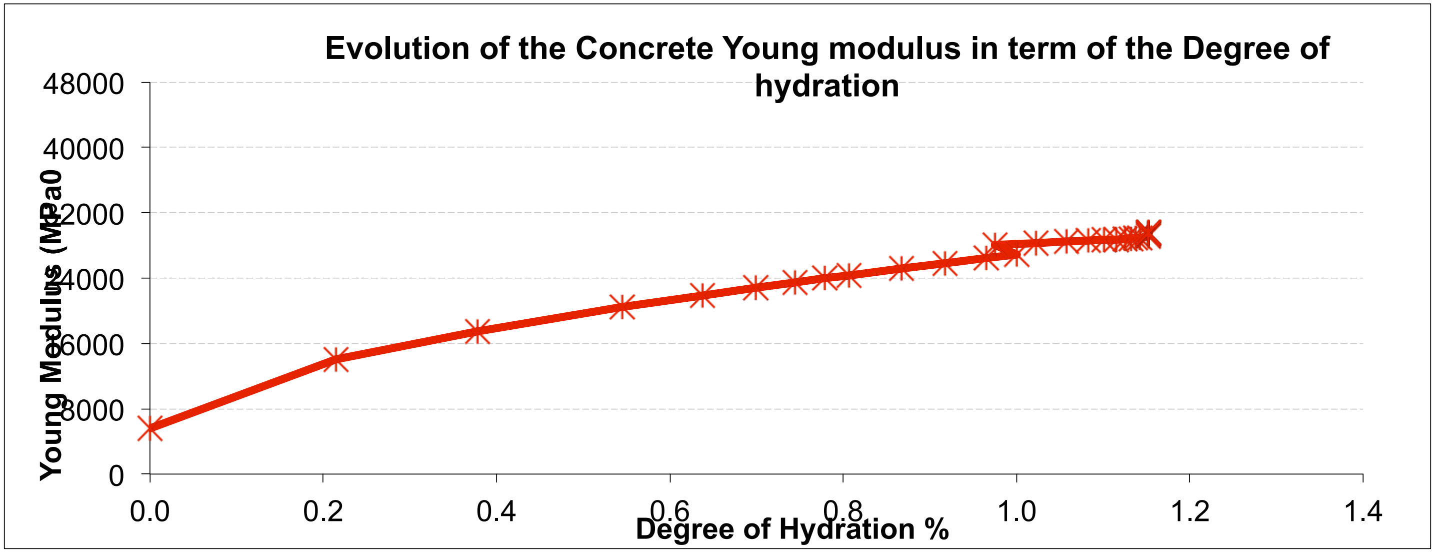

Concrete behavior Modeling

- Thermal effects: $\varepsilon_{T°}$: cooling of the concrete (ΔT = 40°C)
- Concrete Hydration (Hardening) : according to EC2
- Autogeneous effects : $\varepsilon_{autogeneous°}$: according to EC2
- Creep effects: $\varepsilon_{creep°}$: according to EC2

Code_Aster:

Creep Law of Granger:

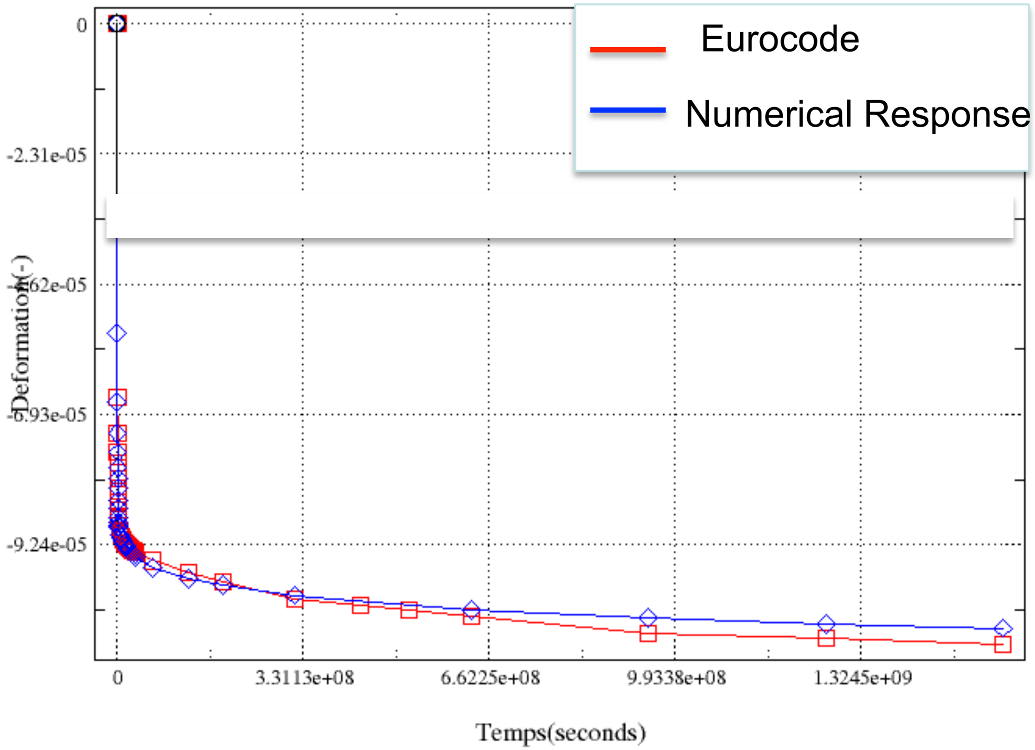

Calculation process

Thermic Computation → ~~Drying Computation~~ → Mechanical Computation

Variation of T (time)

Variation of xxx (time)

Activation of the various effects (time)
At each stage : thermic, hydratation, …

At each lift :
Activation of the new group element
Accounting by the imposed displacement
Of the part already constructed

Activation of all the proprieties after setting of the concrete

Magnification Factor =500

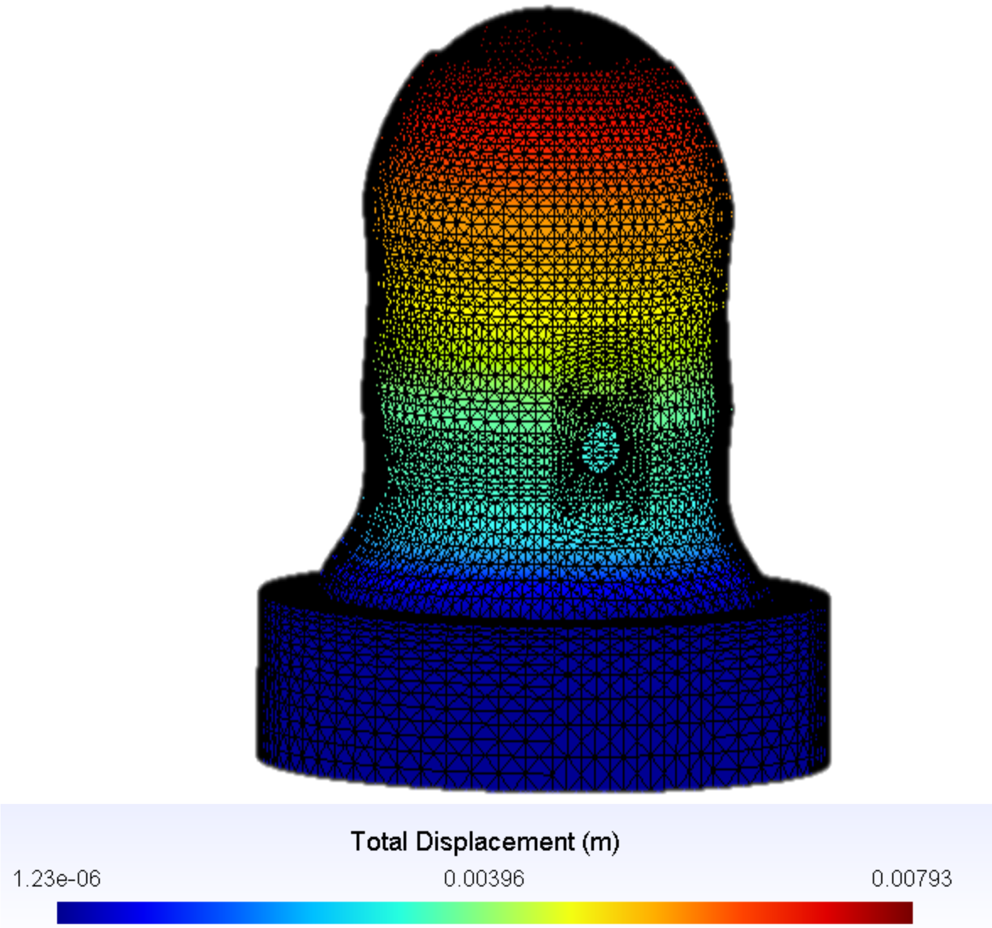

With construction staging

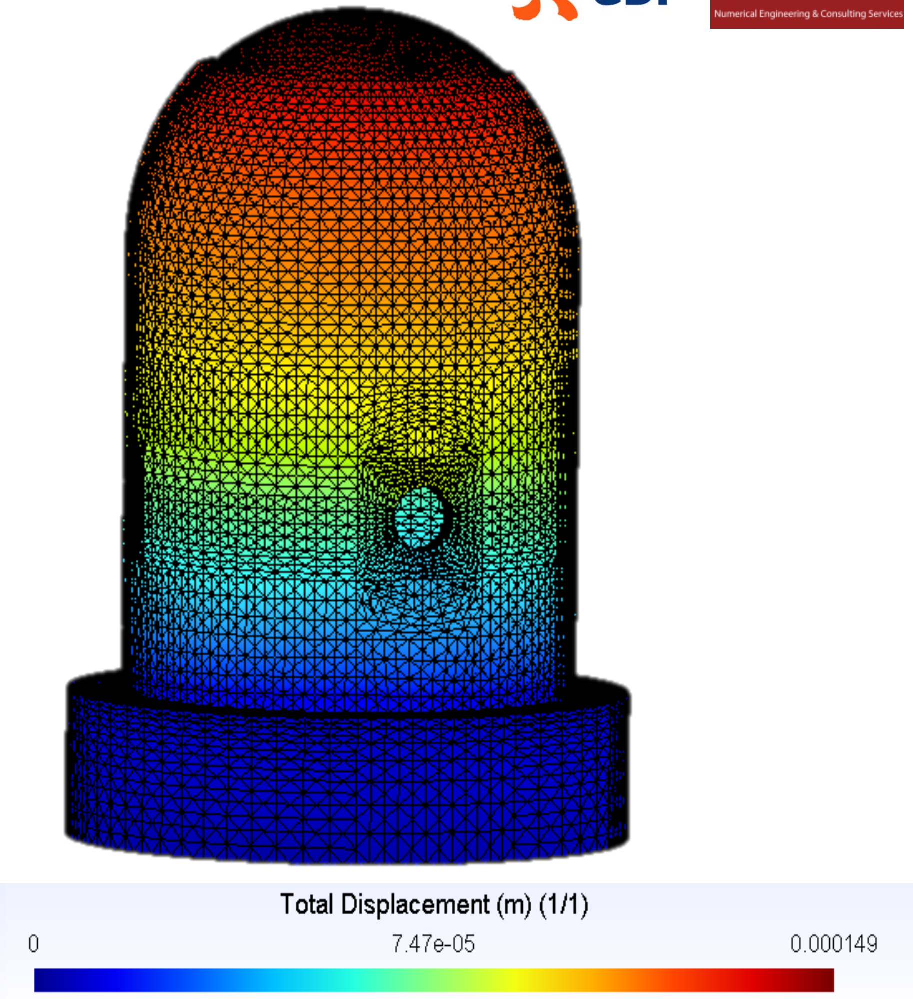

Without construction staging

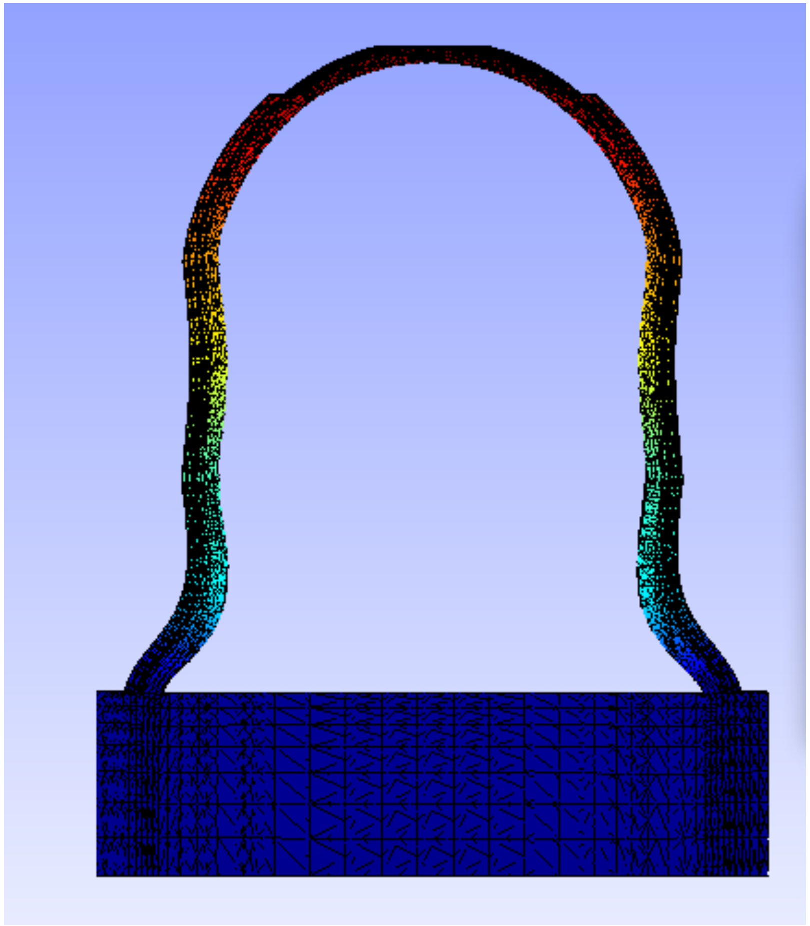

Stress Profiles at 6 months (Inner surface)

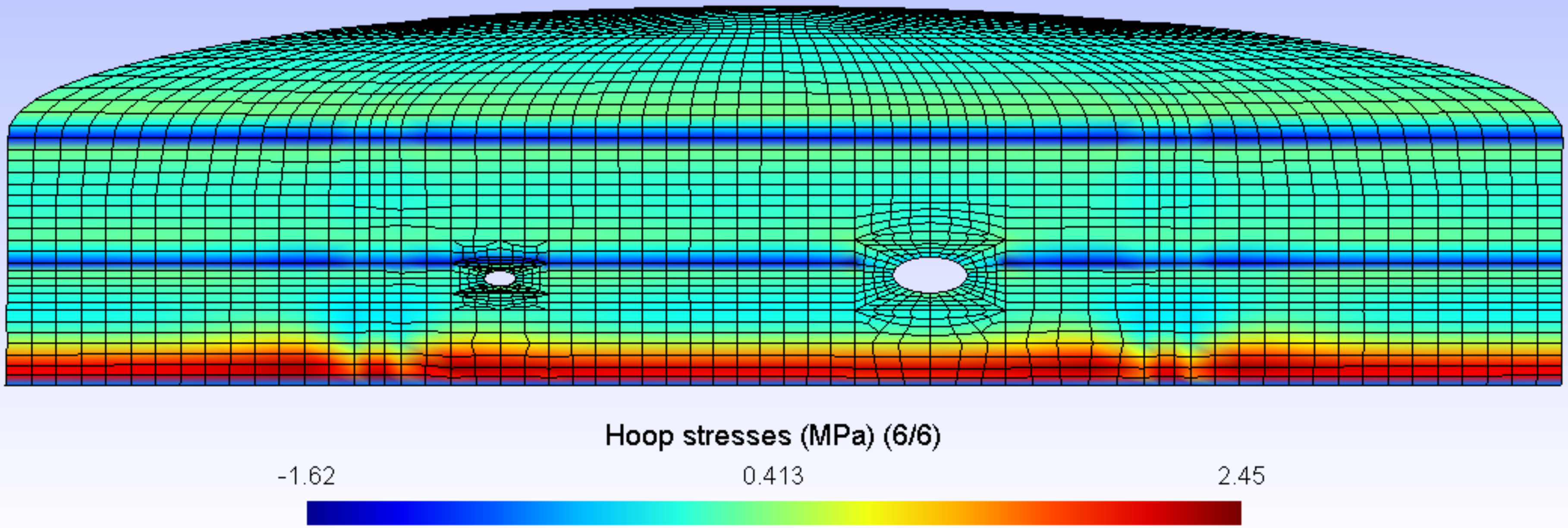

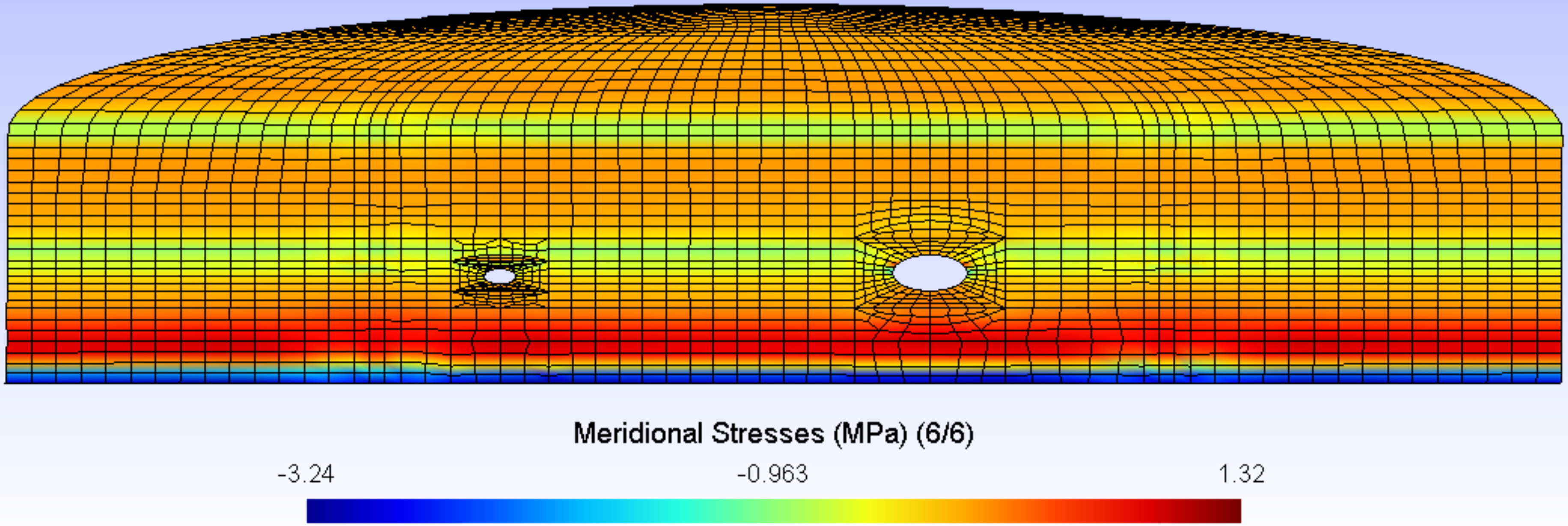

For Azimut 135 °

Hoop stresses distribution over the structure height

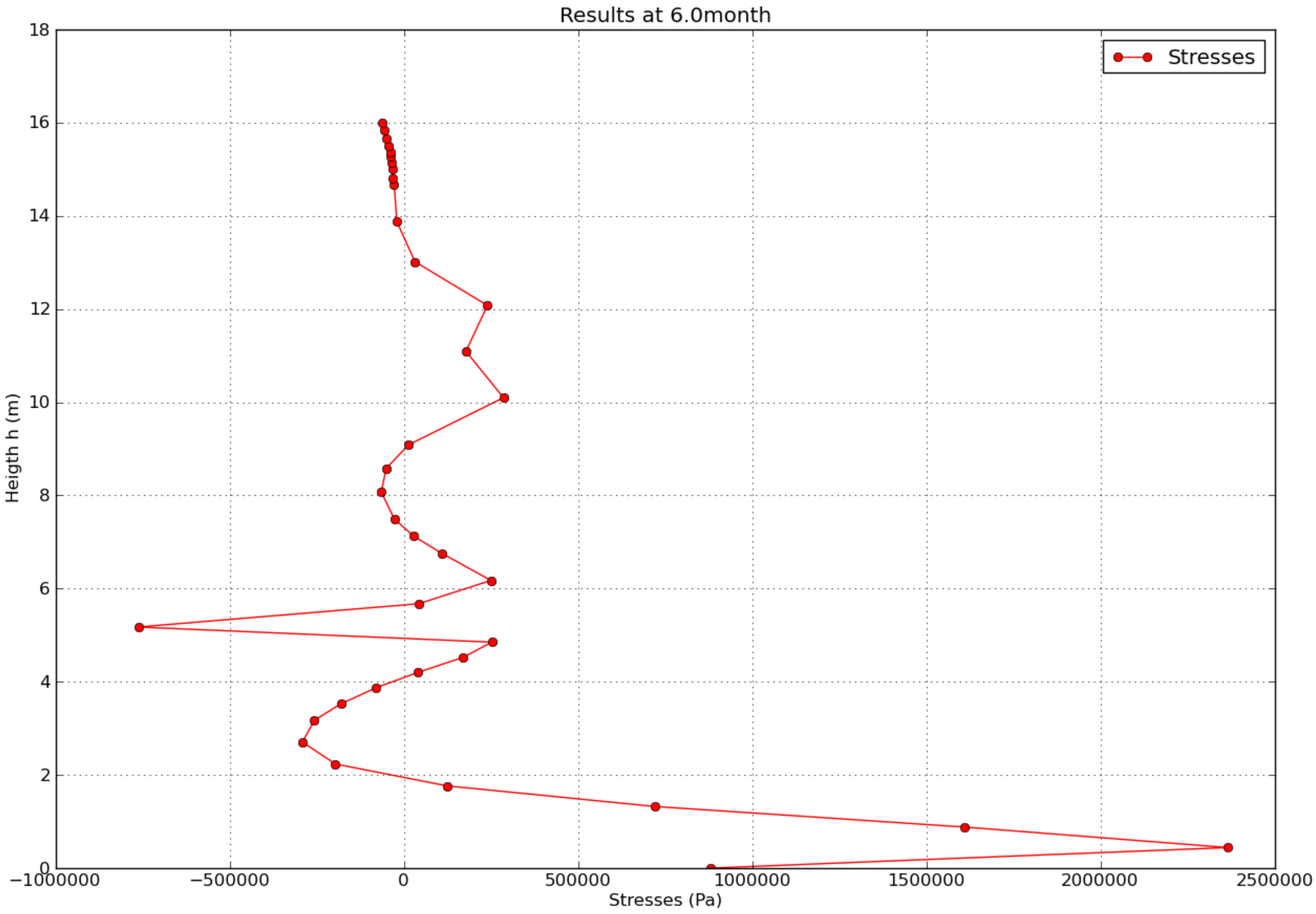

Hoop strains decomposition over the structure height

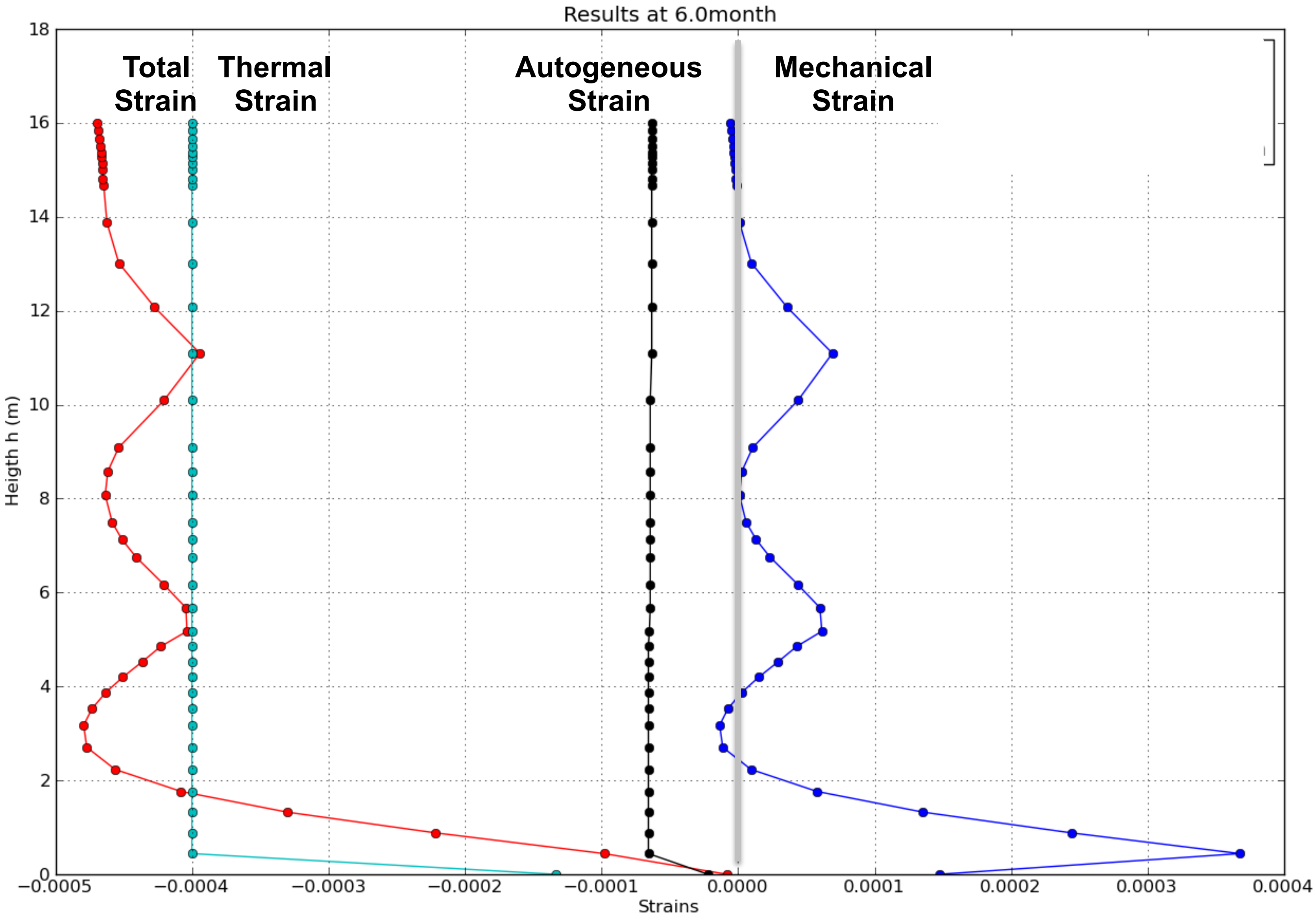

Conclusions

- Interest of studying the different effects intervening in the setting of concrete:
  creep, hydratation, young age

- Stresses map at initial state different from the unstressed initial state assumption

- Future interest in more precise modeling of the phasing construction:
  drying effects w/wo with creep effects.
  account for the progressive prestressing of the cables
  use as initial state for LST test

3. Permeability of the concrete wall

Objectives :
Estimation of the permeability state of the wall
Comparison between different configurations :
- initial state (permeability of concrete)
- initial state with staging and aging effects (permeability of the concrete damaged)

Modeling :
Complete structures
No modeling of the cables

Results :
Map of gas flow for a given pressure and comparison between different configurations

Hydraulic Equation

$$(1-S_l)\phi\frac{\partial P_g}{\partial t} = -div(-\lambda_P(P_g)grad(P_g))$$

$$\lambda_P(P_g) = \frac{K_g}{\eta_g}P_g$$

$$\begin{cases} P = P^d \text{ sur } \Gamma_1 \\ \lambda_p(P_g)\dfrac{\partial P_g}{\partial n} = f(x,t) \text{ sur } \Gamma_2 \end{cases}$$

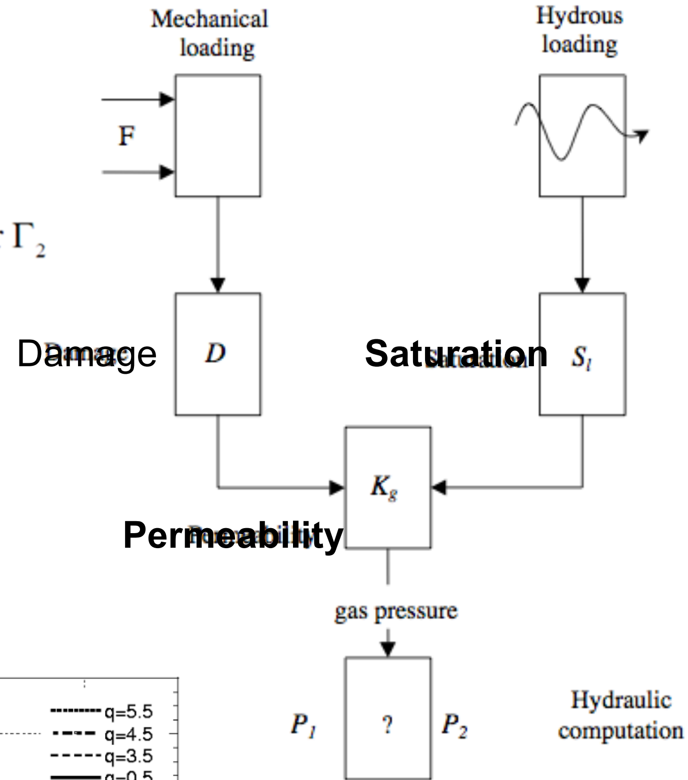

With S_l liquid water degree of Saturation

K_g the gas permeability

Permeability

$$Kg = K_{rg}(S_l) \times K(D)$$

- Relative permeability induced by degree of saturation

$$K_{rg}(S_l) = (1-S_l)^{4.5}(1-S_l^{\,2})$$

$$S_l = \frac{C^{fl}}{C_{sat}}$$

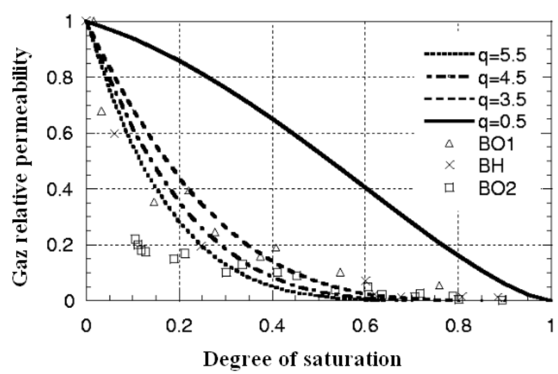

Permeability in term of Degree of saturation

- Permeability induced by damage

$$\begin{cases} K(D) = K_0 & D < 0.035 \\ K(D) = K_0 \times 10^{8.67 \times D - 0.3} & D > 0.035 \end{cases}$$

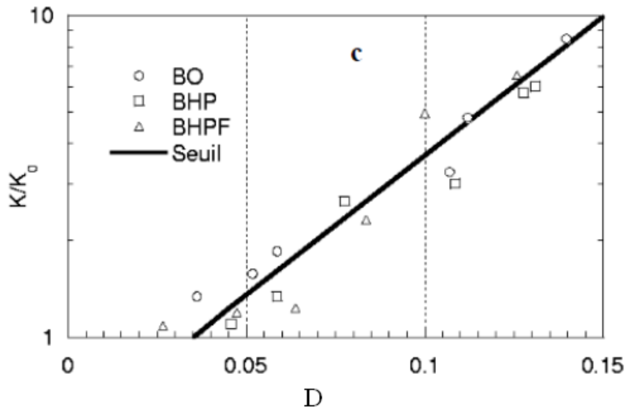

Low damage indices

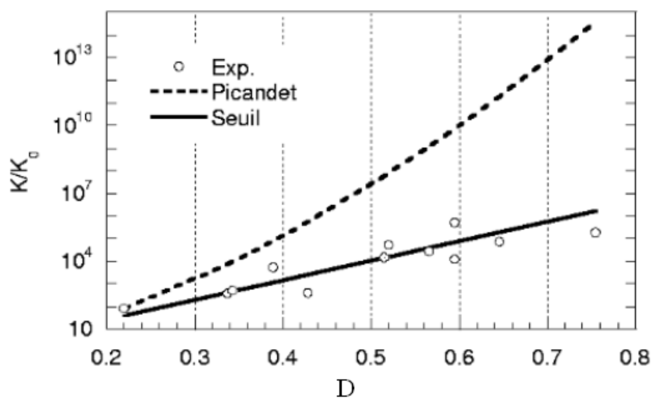

High damage indices

Gas Flow :

$$v_g = -\frac{K(D) \times k_{rg}(S_l)}{\eta_g} grad(P_g) \times \frac{1}{\varphi(1-S_l)}$$

Application

Calculation of leakage rate

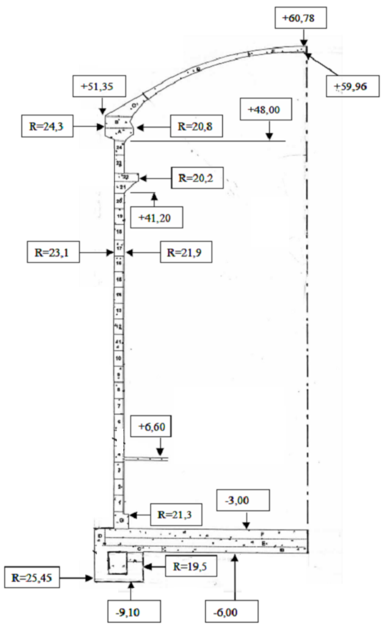

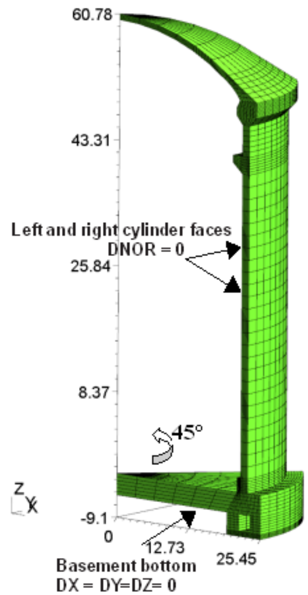

Geometry and modeling of a Vessel

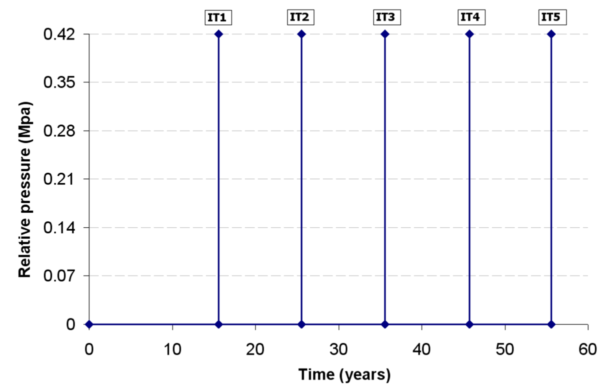

Evolution of the internal pressure during the 60 years

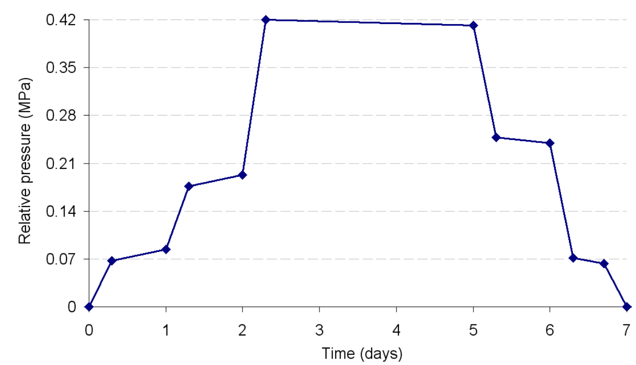

Evolution of the pressure during the test

From Mahsa MOZAYAN KHARAZI

Mechanical Calculation:

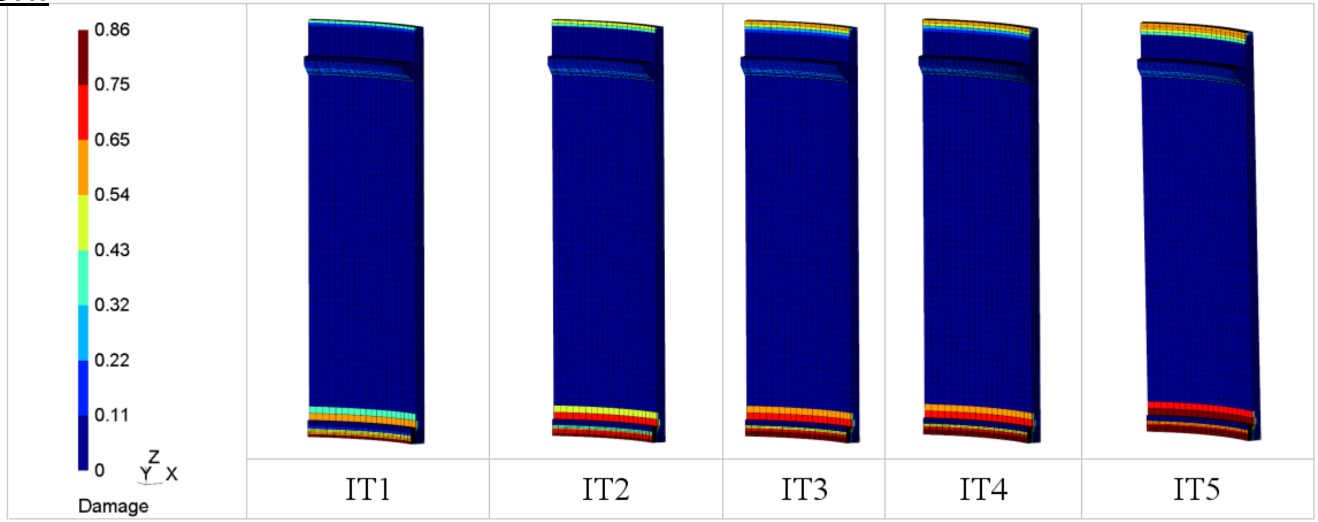

Evolution of the Damage indice at each test

Hydric Calculation:

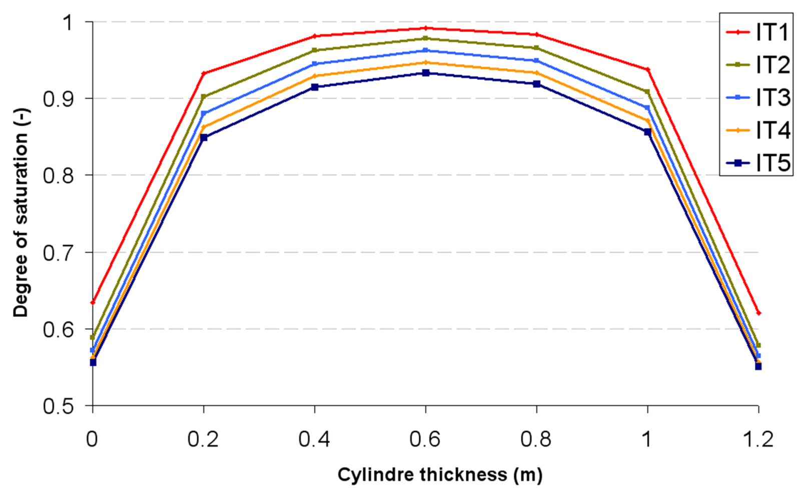

Degree of saturation in the wall thickness for each test

From Mahsa MOZAYAN KHARAZI

Hydraulic Calculation :

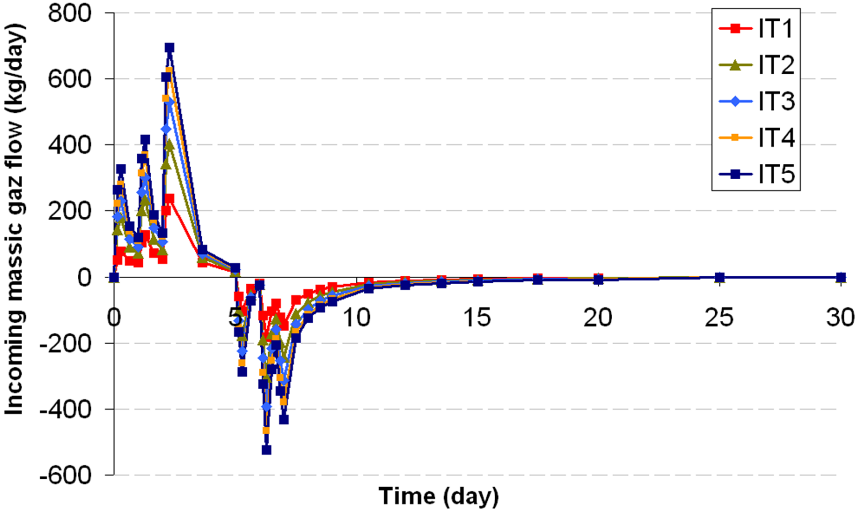

Incoming massic gaz flow during tests

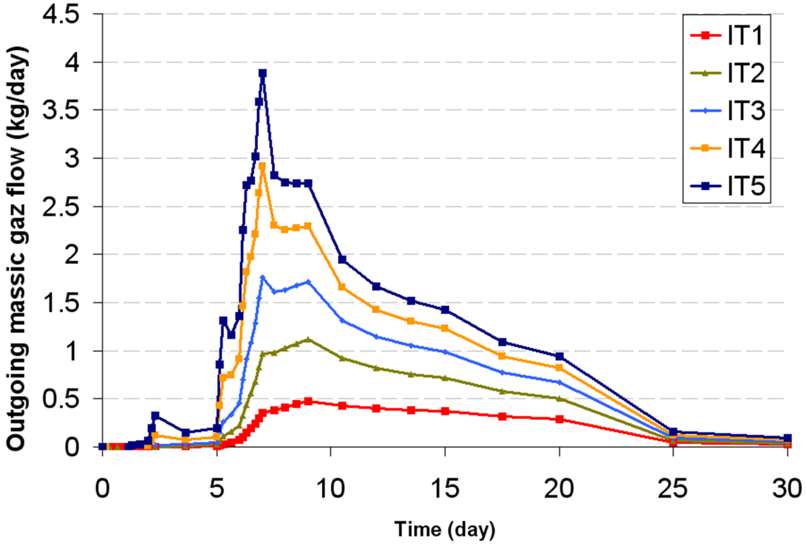

Outgoing massic gaz flow during the tests (effect of the increasing damage)

From Mahsa MOZAYAN KHARAZI

Application to the case of SANDIA: qualitative results

- the deformations obtained with the model with staging after 1 year

↓

Estimation of the local damage using Mazars

$$\sigma_{ij} = (1 - D) C_{ijkl}\, \varepsilon_{kl}$$

$$D = \alpha_t D_t + \alpha_c D_c$$

$$\alpha_{t,c} = \left(\sum_{i=1}^{3} \frac{<\varepsilon_i^{t,c}><\varepsilon_i>_+}{\varepsilon_{eq}^2} \right)^{\beta} \quad D_{t,c} = 1 - \frac{\varepsilon_{eq0}(1 - A_{t,c})}{\varepsilon_{eq}} - \frac{A_{t,c}}{\exp[B_{t,c}(\varepsilon_{eq} - \varepsilon_{eq0})]}$$

$$\varepsilon_{eq} = \sqrt{\sum_{i=1}^{3} (<\varepsilon_i>_+)^2}$$

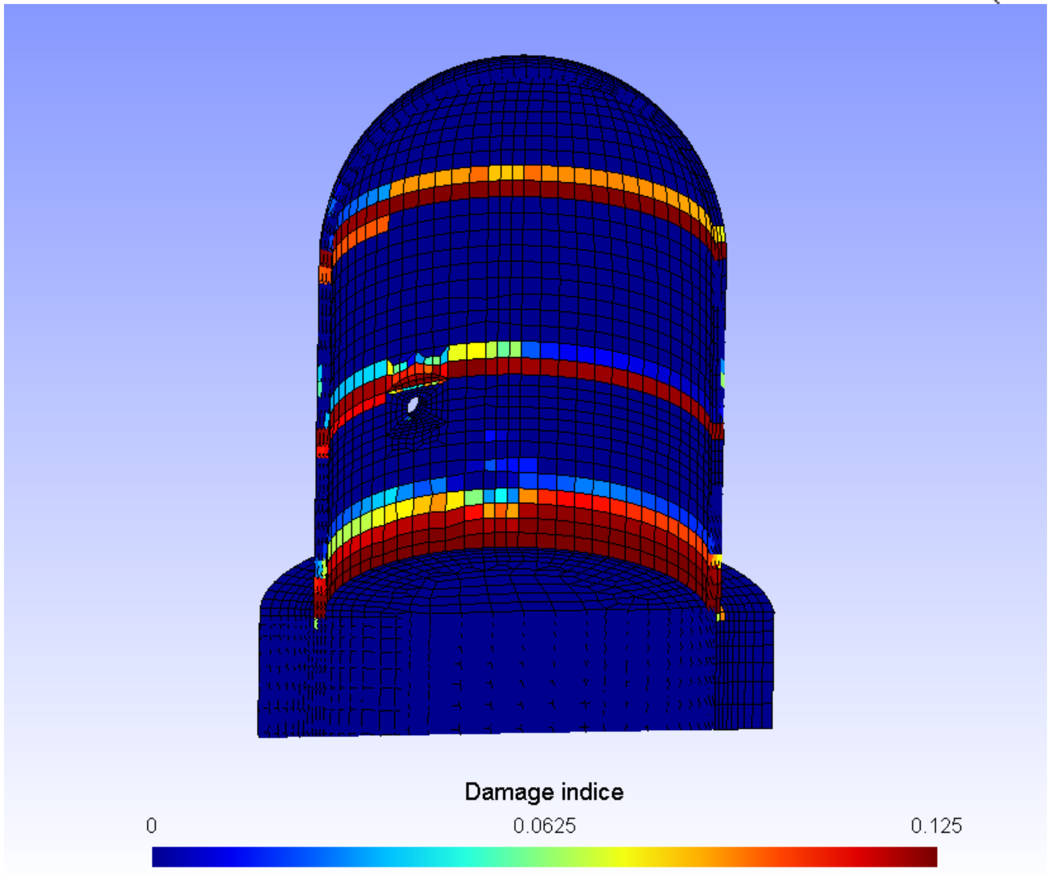

- Saturation Hypothesis: Degree of Saturation :80%

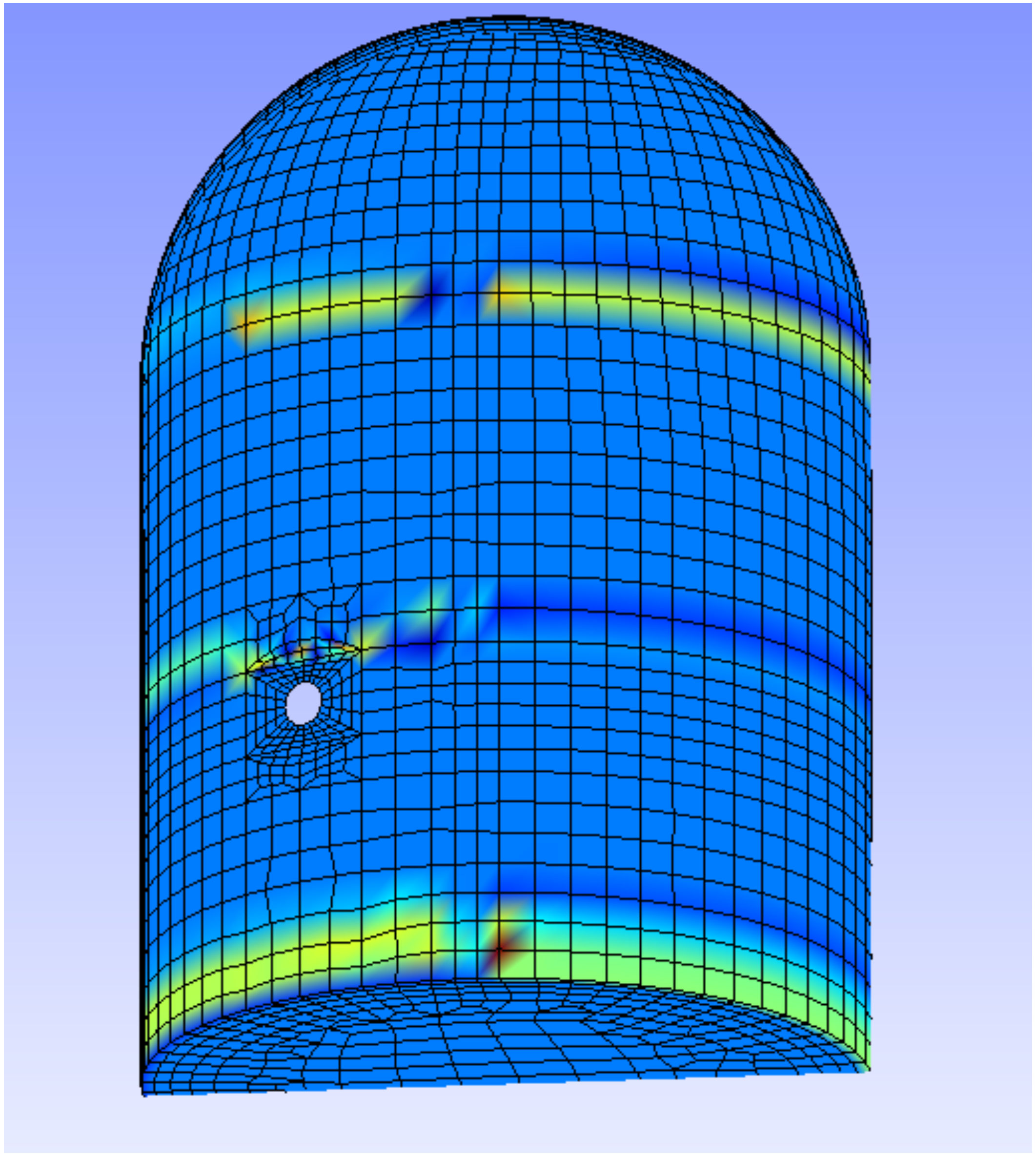

Leakage Map of the inner surface at a given pressure

Conclusions

- Development of a uncoupled thermo-hydro-mechanical methodology to compute leakage rate for containment without liner

- The method allows for measuring the effect of the degree of saturation and progressive damage

- Limitations of the model for law damage structures. Improvement required for large cracks.

4. Rupture of the Liner

Objective :

Model the rupture of the liner with Cohesive Zone Model elements

Modeling :

Sub-structuration :
- Extraction of the displacement field on the liner from the complete structural model.
- Application of the resulting displacements on certain zones of the liner.
- Study of the Liner response with 3 possible tears.

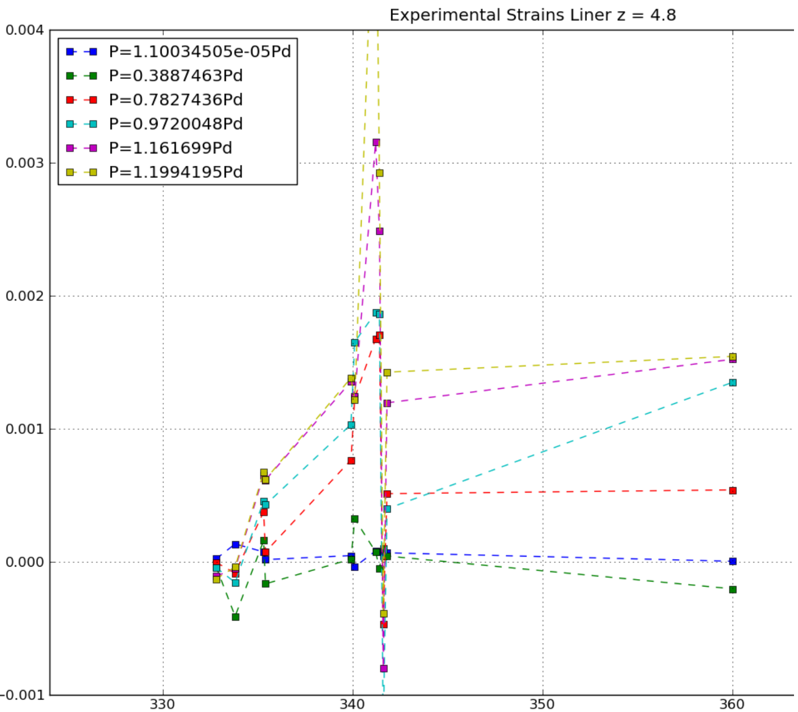

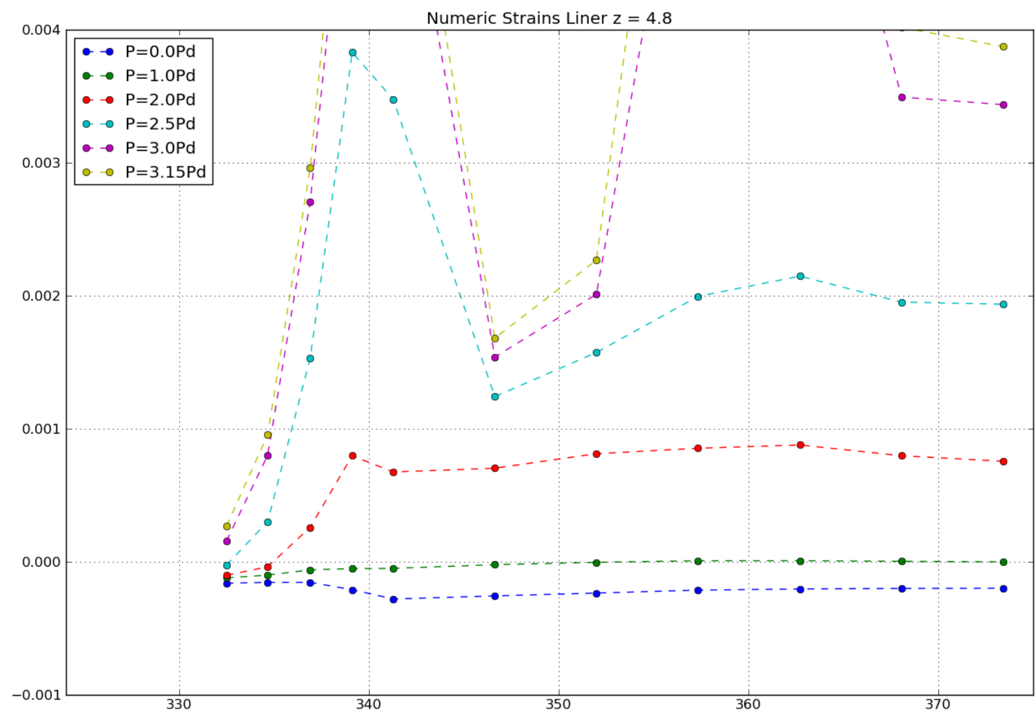

Comparison Liner Hoop strains Experimental versus Numerical close to the E/H at the elevation 4.8

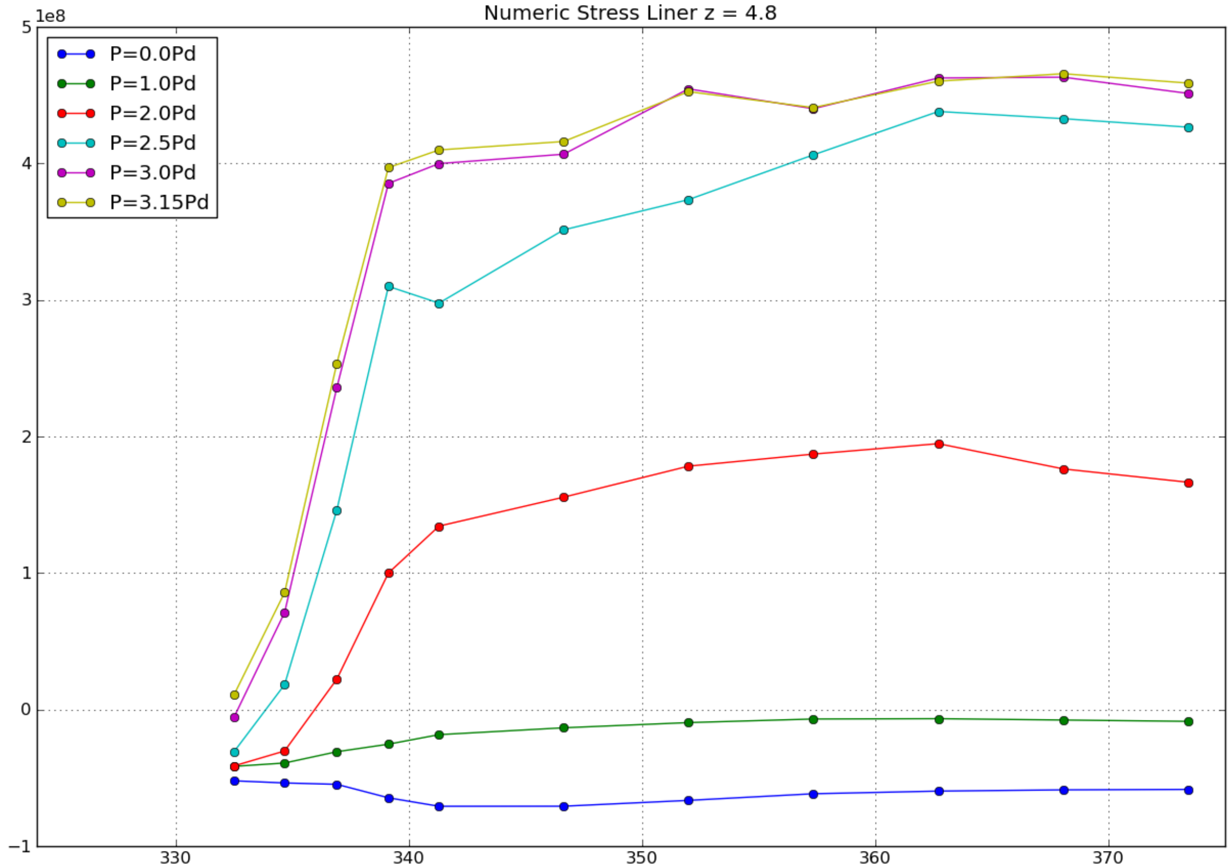

Liner hoop stresses close the E/H hatch at an elevation 4.8m

Meshing: liner

Solid element

Quadratic

Thickness 1.6mm

Liner perfectly bonded with concrete at nodes except around seal lines

Properties: same as for model 1

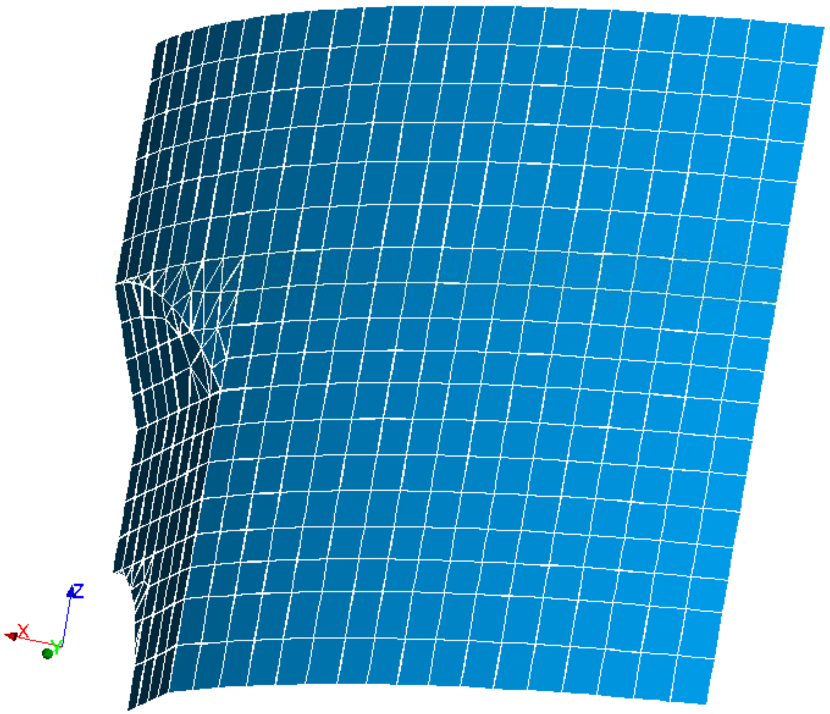

Meshing: seal

Cohesive zone model elements

Hexa-CZE (zero volume element)

Quadratic number of nodes with special shape function

Liner / concrete interface: same radial displacement

E= 223 GPA

ν= 0

ρ= 7 850 kg/m^3

GC = 130 MPa.µm — Surface energy density

SIGM_C = 400 MPa — Failure stress

COEF_EXTR =0.

COEF_PLAS = 0.5 — Shape of stress vs jump displacement curve - Mode I crack opening

Seals surrounding the E/H

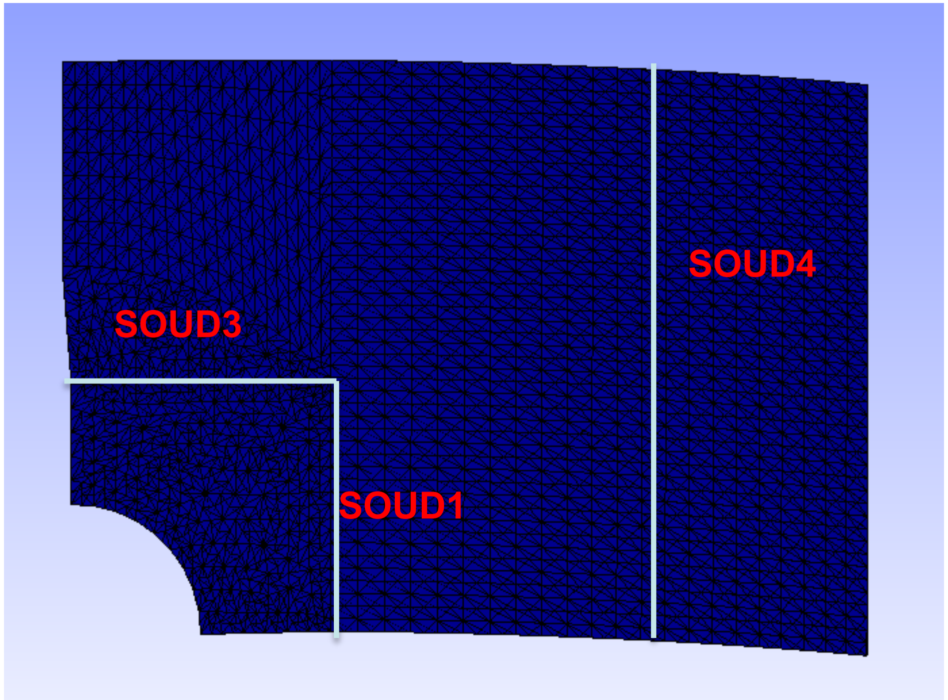

Cohesive zone model elements

Example of tetra-cohesive zone elements with opening in Mode I

The cohesive law for ductile fracture

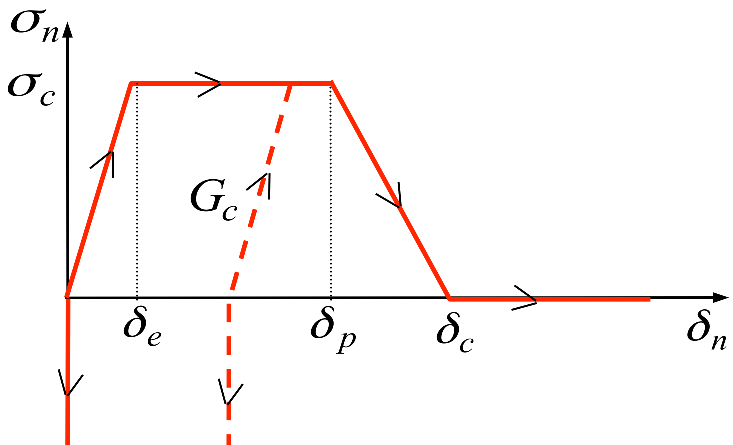

$$\sigma_n(\delta_n) = \sigma_c \begin{cases} \dfrac{\delta_n}{\delta_e} & \text{if} \quad \delta_n \le \delta_e \\ 1 & \text{if} \quad \delta_e < \delta_n < \delta_p \\ \dfrac{\delta_c - \delta_n}{\delta_c - \delta_p} & \text{if} \quad \delta_p \le \delta_n < \delta_c \\ 0 & \text{if} \quad \delta_n \ge \delta_c \end{cases}$$

$$\delta_c = 2G_c/\sigma_c + \delta_e - \delta_p \qquad \delta_e \le \delta_p < \delta_c$$

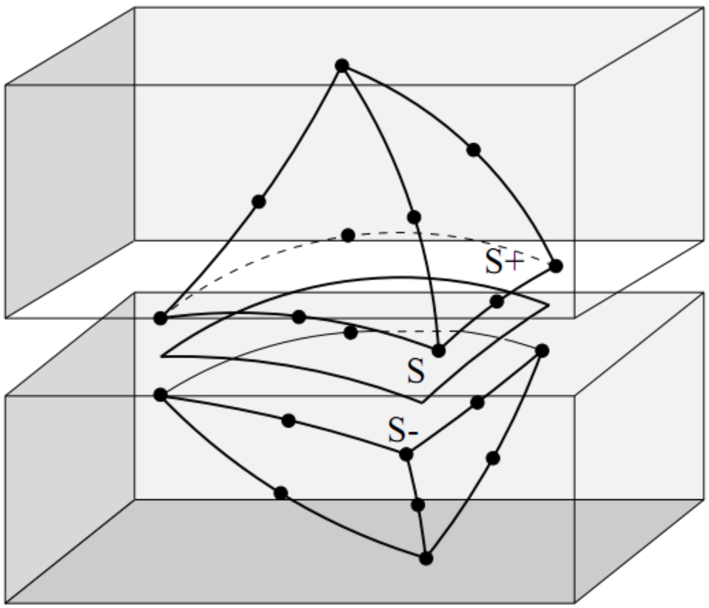

Assembly of a cohesive element with adjacent liner elements

Deformed shape of the liner

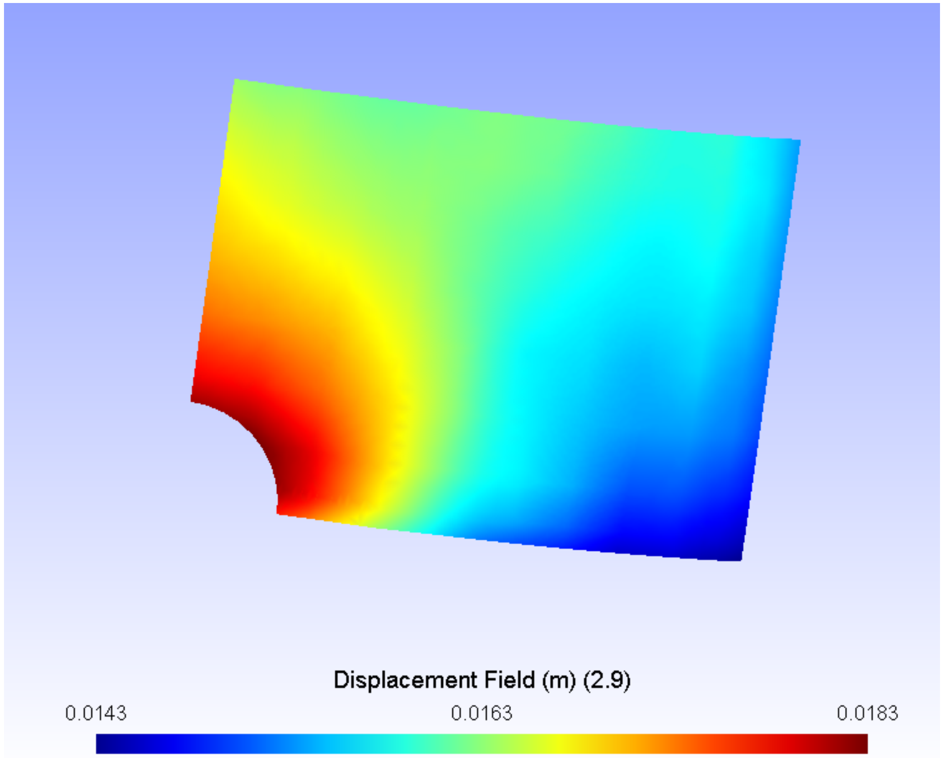

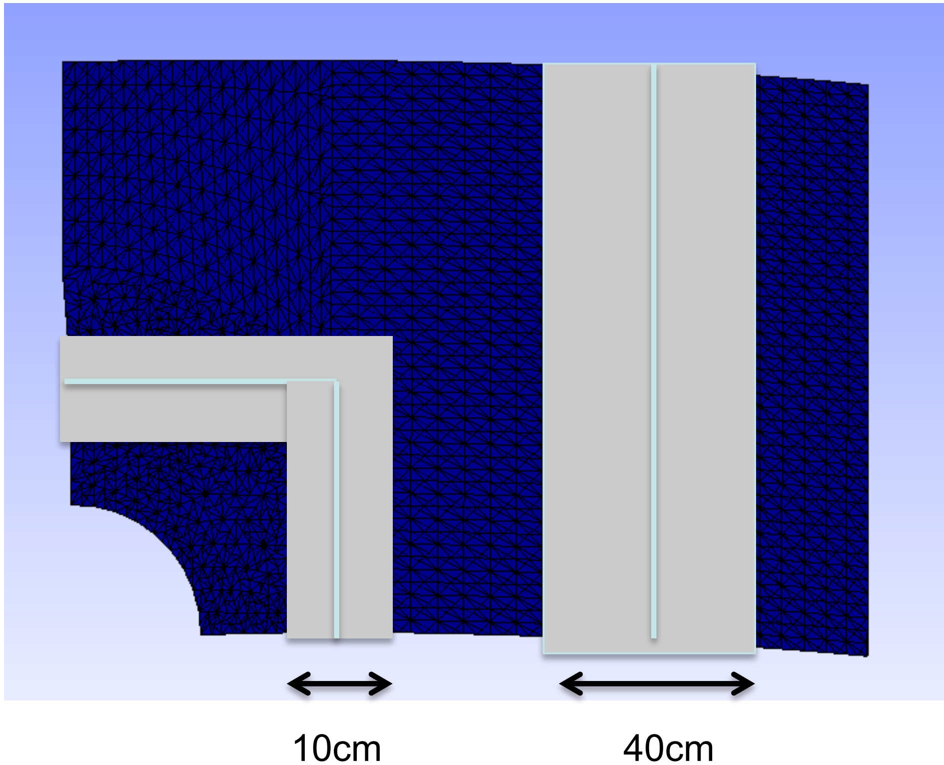

Application of the displacement on the liner.

From the zone close to the cohesive zone,
the radial displacement of the liner is imposed

Magnification Factor =10

Visualization of the opening of the seals at P=2.9Pd

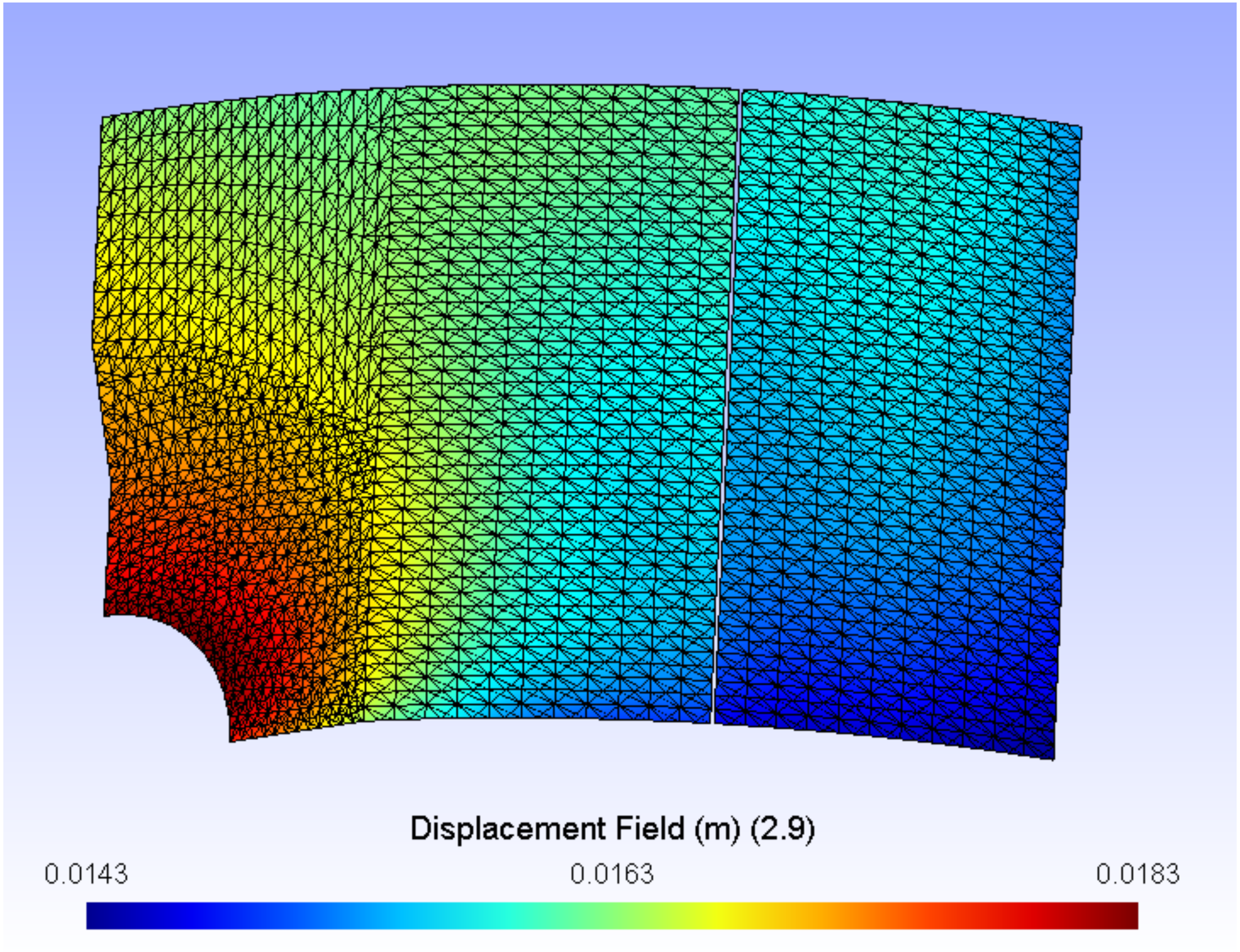

Displacements of the seal lips at P =2.85Pd

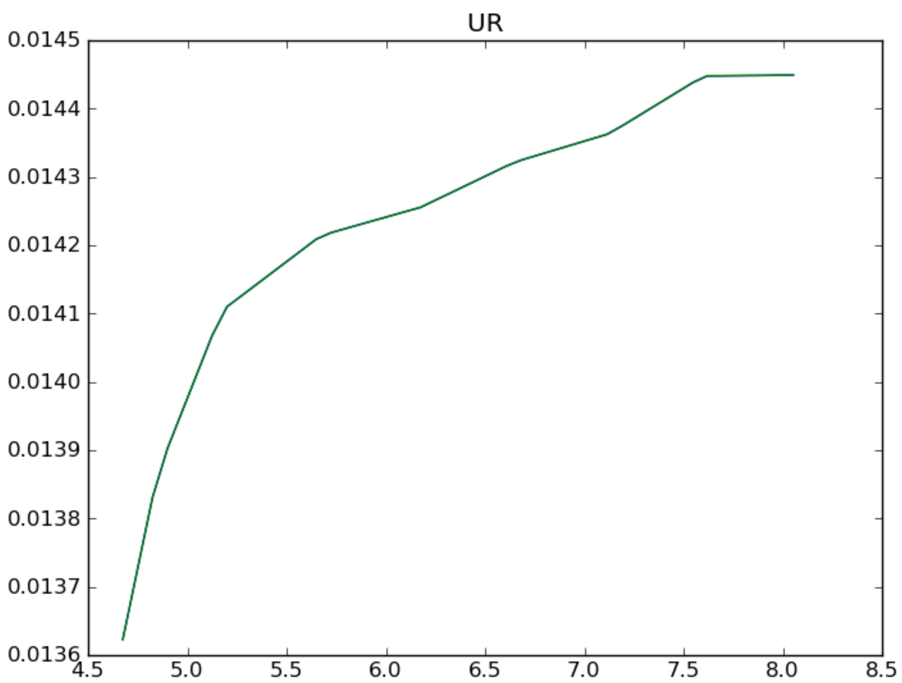

Variation of Radial Displacement over the height of the seal

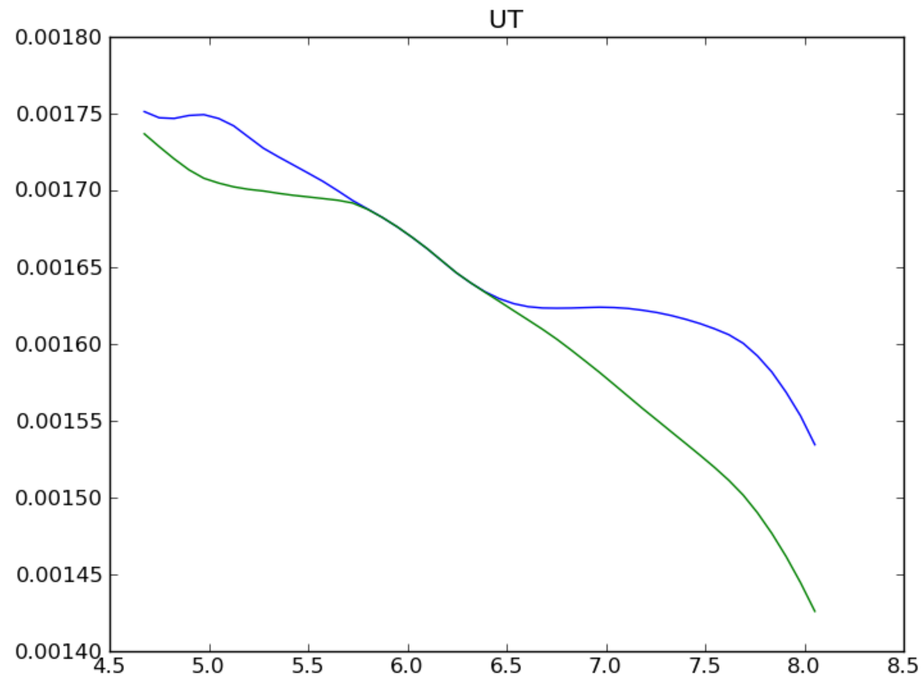

Variation of Hoop Displacement over the height of the seal SOUD4

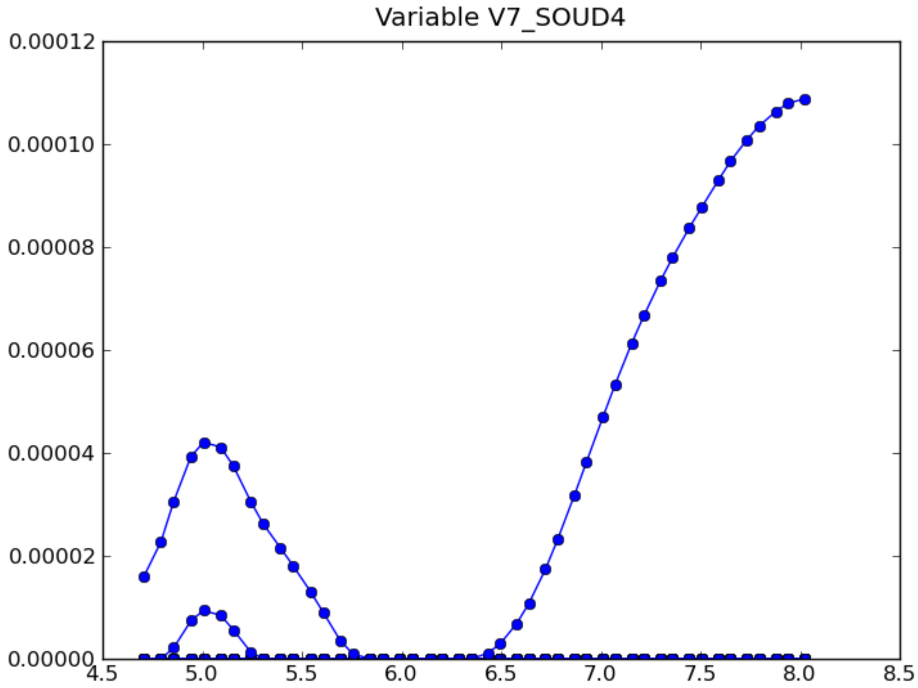

Opening of the **SOUD 4:**
Measure of the displacement jump along the seal length

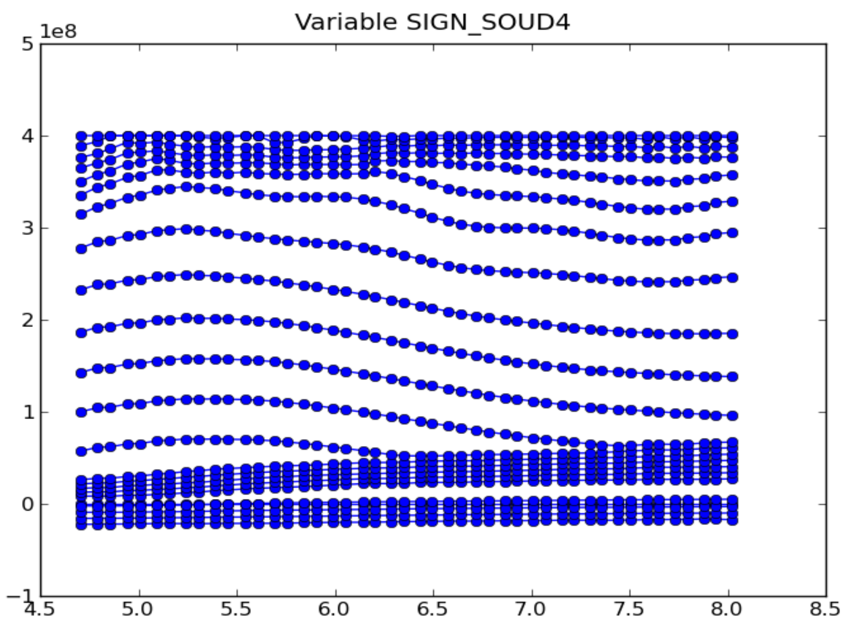

Normal stress in the cohesive zone elemen
along the seal length

A1

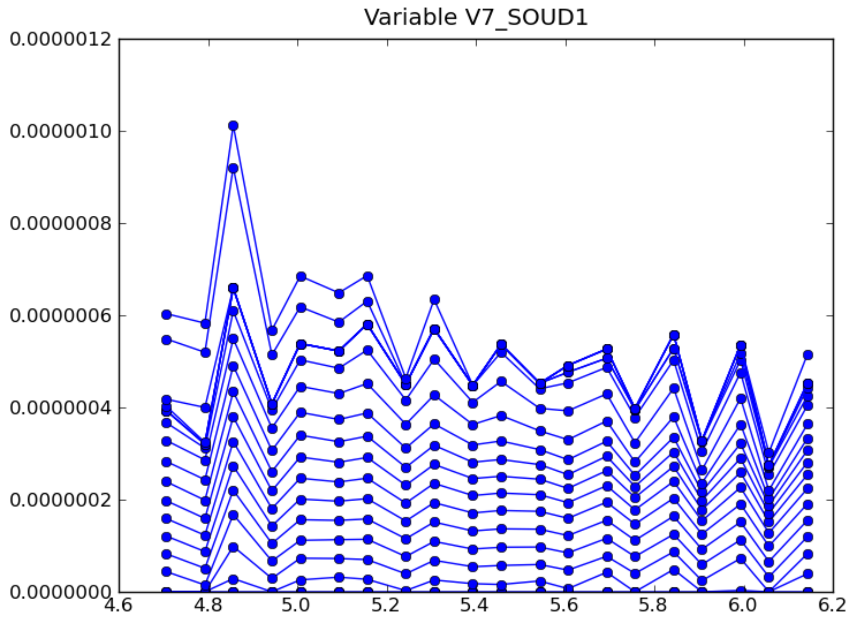

Opening of the **SOUD 1**:
Measure of the displacement jump along the seal length

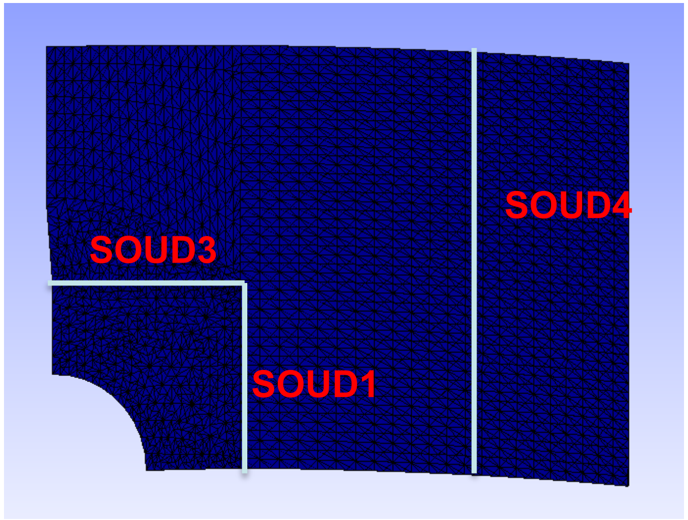

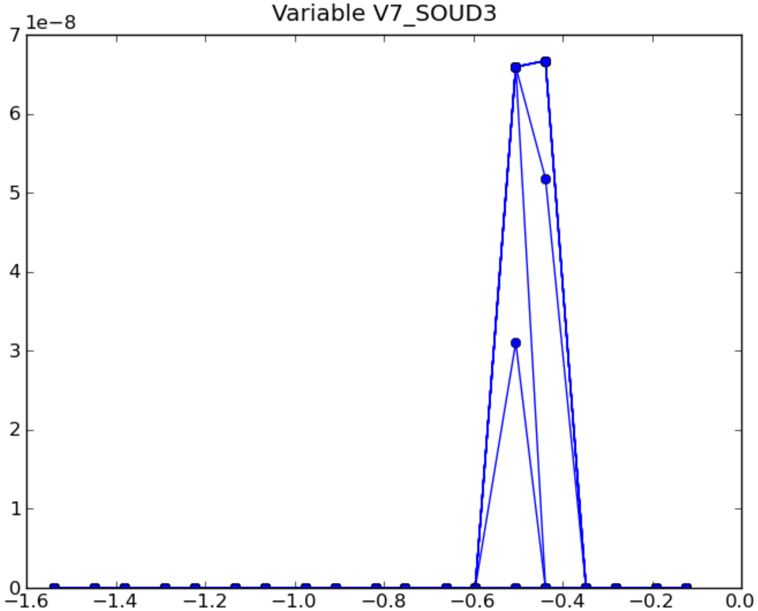

Opening of the **SOUD 3**:
Measure of the displacement jump along the seal length

Conclusions

Promising results of Application of the CZM to the rupture of the Liner:

- Activation of the various seals.
- Progressive opening of the seal

Limitations and problems to overcome:

- Sensitivity to the refinement of the mesh / parameters
- Sensitivity to the methodology (displacements imposed)
- Overcome convergence problems related to the softening behavior of the CZM law